Supporting Information

Photoswitchable glycoligands targeting *Pseudomonas aeruginosa* LecA

Y. Fan,[a] A. El Rhaz,[b] S. Maisonneuve,[a] E. Gillon,[c] M. Fatthalla,[c] F. Le Bideau,[c] G. Laurent,[a] S. Messaoudi,[d] A. Imberty,*[c] and J. Xie*[a]

[a] Photophysique et Photochimie Supramoléculaires et Macromoléculaires, University Paris-Saclay, ENS Paris-Saclay, Alembert Institute, CNRS, 91190, Gif-sur-Yvette, France
[b] Université Paris-Saclay, CNRS, BioCIS, 92290, Orsay, France
[c] CERMAV, University Grenoble Alpes, CNRS, 38000 Grenoble, France
[d] Laboratoire de Synthèse Organique, Ecole Polytechnique, CNRS, ENSTA, Institut Polytechnique de Paris, 91128 Palaiseau, France

E-mail: anne.imberty@cermav.cnrs.fr, joanne.xie@ens-paris-saclay.fr

1. General Methods

Photochromic reactions were induced *in situ* by a continuous irradiation Hg/Xe lamp (Hamamatsu, LC6- or LC8-Lightningcure, 200 W) equipped with narrow band interference filters of appropriate wavelengths Semrock FF01-370/36 for λ_{irr} = 370 nm; Semrock FF01-438/24-25 for λ_{irr} = 438 nm; Semrock FF01-485/20-25 for λ_{irr} = 485 nm. The incident lamp power was measured by means of an Ophir PD300-UV photodiode. NIR contribution (P_{LP}) has been measured and subtracted from the total value using Schott long pass filter LP-545 nm for irradiations at 370 nm, 438 nm and 485 nm that is let through the Semrock filter (P_{Total}), and considering a 90% transmittance: $P_{\lambda irr} = P_{Total} - (10/9 \times P_{LP})$.

The photoconversion yields were measured from a solution of compound in deuterated solvent and monitored by ^{1}H NMR and UV-visible absorption, after successive irradiations at 370 nm (438 nm or 485 nm) in the case of the PSS. The *E/Z* ratios were determined by integration of characteristic of each isomer.

Data processing of spectroscopic measurements was realized with the help of Microsoft® Excel® and Igor Pro from WaveMetrics, Inc (versions 7 to 9).

2. Detailed photochemical and photophysical procedures

2.1.Determination of the molar absorption coefficients (ε)

A mother solution of compound (*E*)-**1** was freshly prepared in H_2O in a precise concentration (C = 0.219 mmol·L^{-1}; 0.301 mg dissolved in 3000 µL). From the mother solution, a series of 7 to 10 daughter solutions were prepared with a concentration range from 2 µM to 37 µM, and their absorbance was measured independently by UV-Vis absorption at room temperature (20 to 23 °C).

To ensure the reproducibility and evaluate the accuracy of the measurements, each recorded spectrum was divided by its concentration in order to obtain the corresponding normalized spectrum; only the overlapped normalized spectra are used for the determination of the molar absorption coefficient. Then, the absorption was taken at the maximum of wavelength (353 nm) to calculate the molar absorption coefficients by a linear regression fitting using the least squares method and with a forcing to pass through the origin of coordinates.

The molar absorption coefficient is calculated according to the BEER-LAMBERT law,

$$A(\lambda) = \varepsilon(\lambda) \cdot l \cdot C$$

with

$A(\lambda)$, represents the absorbance at the wavelength λ
$\varepsilon(\lambda)$, represents the molar absorption coefficient at the wavelength λ, in mol·L^{-1}·cm^{-1}
l, the distance of the trajectory in the media, in cm
C, the concentration of the substrate in mol·L^{-1}

Epsilon of the compound E-1

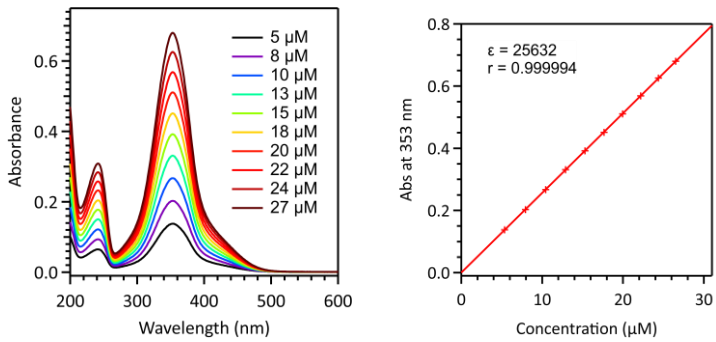

Figure S1. UV-Vis absorption spectra of *E*-**1** measured in H_2O for the daughter solutions (left) and evolution of the absorbance (right) as function of the concentration at the maximum of wavelength (353 nm). Mother solution: 0.301 mg dissolved in 3000 µL of H_2O (C = 0.219 mmol·L^{-1}).

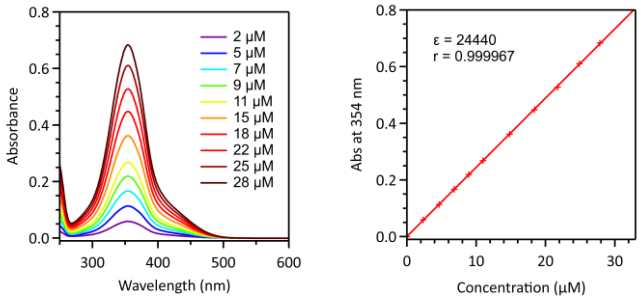

Figure S2. UV-Vis absorption spectra of *E*-**1** measured in Tris buffer: DMSO (95/5) for the daughter solutions (left) and evolution of the absorbance (right) as function of the concentration at the maximum of wavelength (354 nm). Mother solution: 0.165 mg dissolved in a mixture solution of 150 µL DMSO and 2850 µL buffer (C = 0.121 mmol·L^{-1}).

Epsilon of the compound E-2

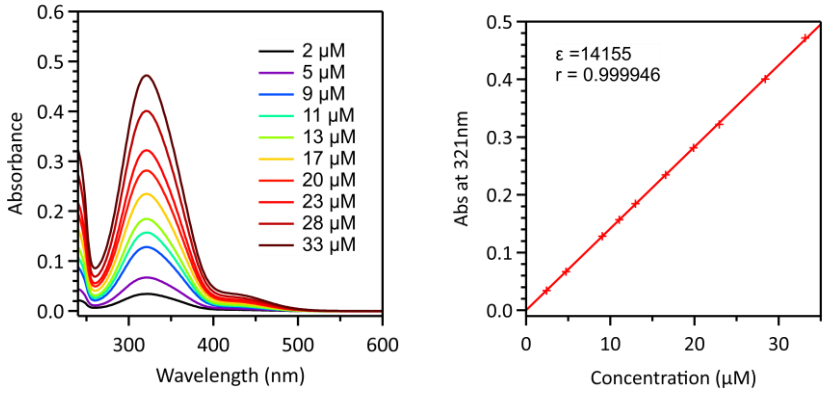

Figure S3. UV-Vis absorption spectra of *E*-**2** measured in Tris buffer: DMSO (95/5) for the daughter solutions (left) and evolution of the absorbance (right) as function of the concentration at the maximum of wavelength (321 nm). Mother solution: 0.136 mg dissolved in a mixture solution of 150 µL DMSO and 2850 µL buffer (*C* = 0.099 mmol·L^{-1}).

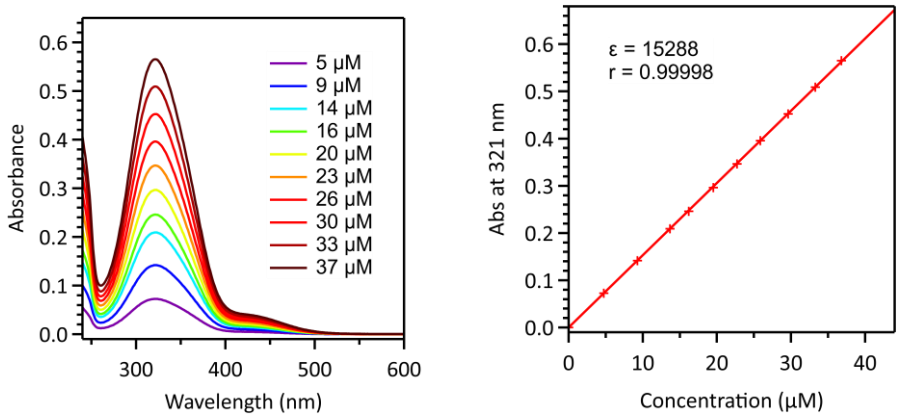

Figure S4. UV-Vis absorption spectra of *E*-**2** measured in Tris buffer: DMSO (9/1) for the daughter solutions (left) and evolution of the absorbance (right) as function of the concentration at the maximum of wavelength (321 nm). Mother solution: 0.220 mg dissolved in a mixture solution of 200 µL DMSO and 1800 µL buffer (C = 0.241 mmol·L^{-1}).

Epsilon of the compound E-3

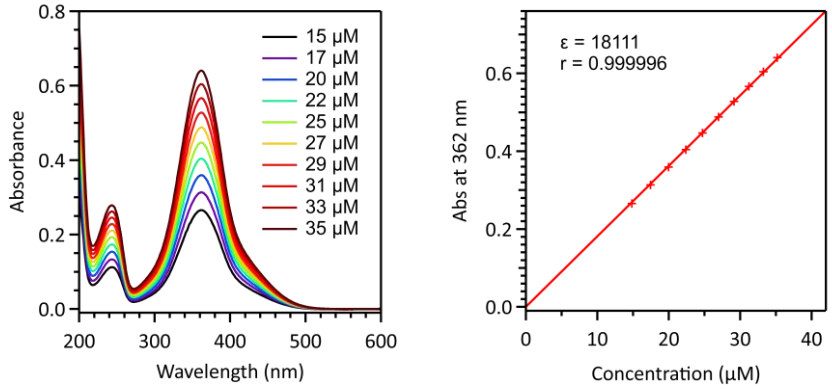

Figure S5. UV-Vis absorption spectra of *E*-**3** measured in H_2O for the daughter solutions (left) and evolution of the absorbance (right) as function of the concentration at the maximum of wavelength (362 nm). Mother solution: 0.210 mg dissolved in 3000 µL of H_2O (C = 0.148 mmol·L^{-1}).

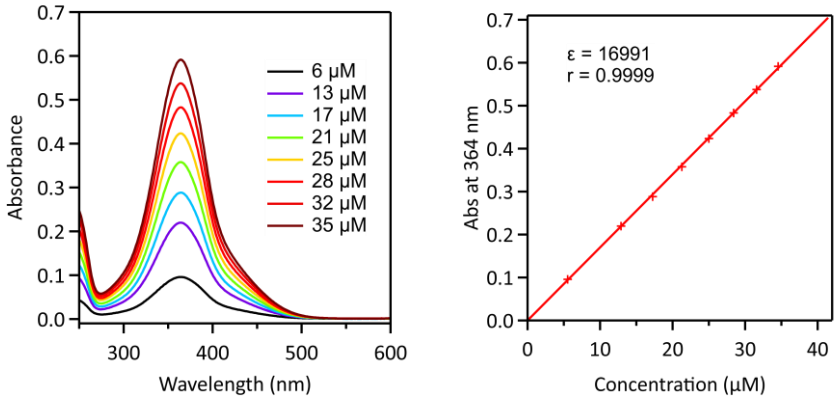

Figure S6. UV-Vis absorption spectra of *E*-**3** measured in Tris buffer: DMSO (9/1) for the daughter solutions (left) and evolution of the absorbance (right) as function of the concentration at the maximum of wavelength (364 nm). Mother solution: 0.164 mg dissolved in a mixture solution of 300 µL DMSO and 2700 µL buffer (*C* = 0.116 mmol·L^{-1}).

Epsilon of the compound E-4

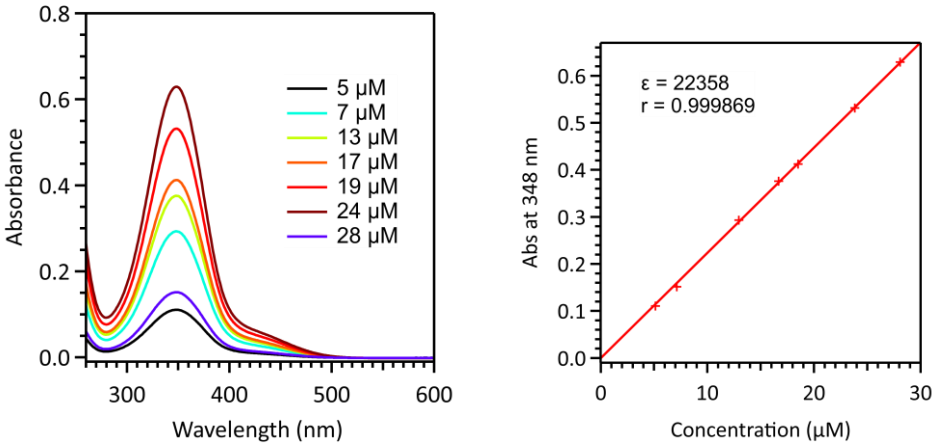

Figure S7. UV-Vis absorption spectra of *E*-**4** measured in Tris buffer: DMSO (9:1) for the daughter solutions (left) and evolution of the absorbance (right) as function of the concentration at the maximum of wavelength (348 nm). Mother solution: 0.371 mg dissolved in a mixture solution of 300 µL DMSO and 2700 µL buffer (C = 0.262 mmol·L^{-1}).

Epsilon of the compound E-5

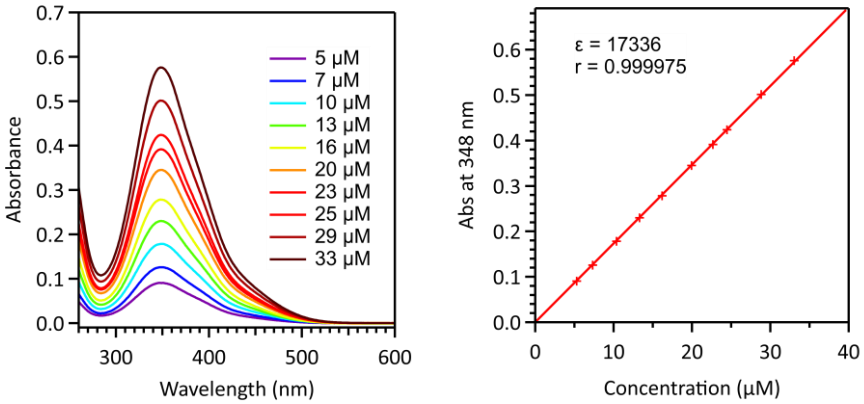

Figure S8. UV-Vis absorption spectra of *E*-**5** measured in Tris buffer: DMSO (9/1) for the daughter solutions (left) and evolution of the absorbance (right) as function of the concentration at the maximum of wavelength (348 nm). Mother solution: 0.254 mg dissolved in a mixture solution of 200 µL DMSO and 1800 µL (C = 0.269 mmol·L^{-1}).

2.2. Determination of the half-lifes

General procedure, illustrated with the case of compound Z-1 half-life in D_2O

The thermal *Z*→*E* isomerization was tracked by measuring UV-Vis absorption spectra at about 22±1°C (room temperature). The obtained time-dependent absorption profiles, taking *Z*-**1** as an example (black cross, **Figure S9**), were fitted with the following first order rate equation:

$$Abs(t) = A_o - (A_o - A_i)e^{-kt}$$

with
A_o, the absorption of original *E*-isomer (holded parameter)
A_i, the absorption at the PSS_{370} (holded parameter)
k, the rate constant of thermal isomerization
t, the time in minutes

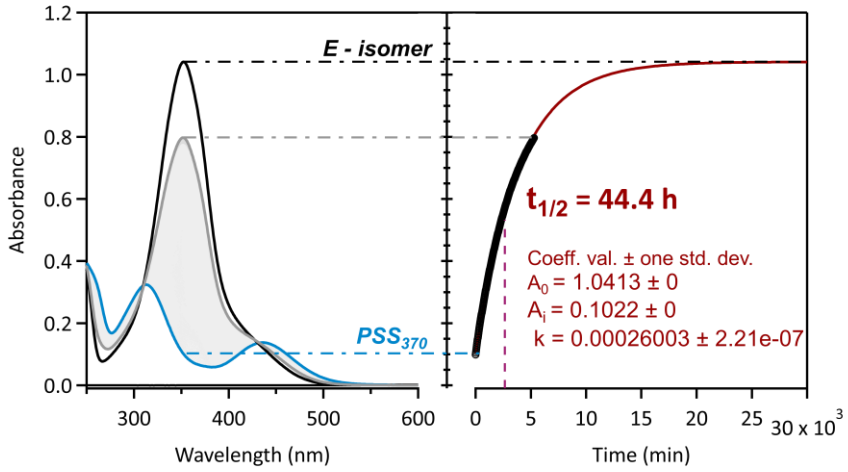

Figure S9: UV-Vis absorption spectra (left) and thermal return monitoring (right) of *Z*-**1** at 352 nm in D_2O at room temperature (≈ 22°C). The reported data points are the result of a single kinetic measurement realized on a solution from the PSS_{370}: 0 to 5300 min (step = 20 min).

After fitting (dark red curve), the rate constant at 22°C (T = 295 K) was obtained from the fitting parameters:

$$k_{295} = 2.6 \times 10^{-4}\ min^{-1}$$

The half-life of *Z*-**1** at room temperature was then calculated:

$$t_{1/2} = \frac{\ln(2)}{k_T}$$

$$t_{1/2} = 2665.6\ min \cong 44.4\ h$$

Similarly, the half-life of *Z*-**2, 3, 4** and **5** was estimated by this method.

Half-life of compound Z-2 in Tris buffer/DMSO (95/5)

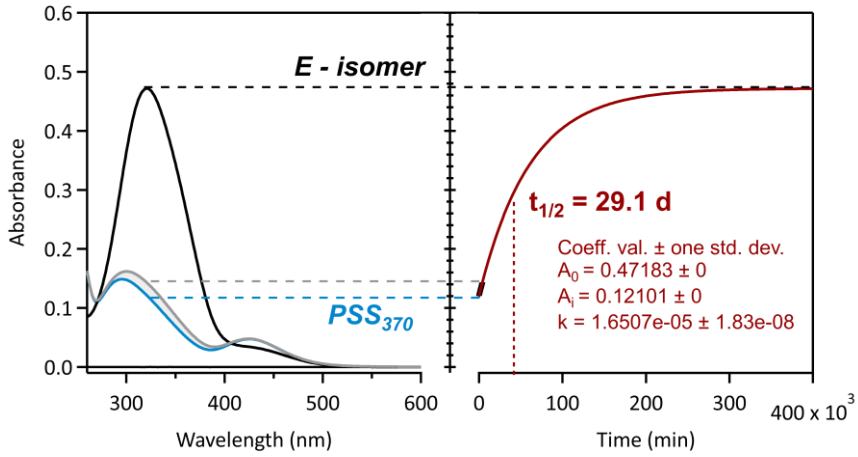

Figure S10: UV-Vis absorption spectra (left) and thermal return monitoring (right) of *Z*-**2** at 321 nm in Tris buffer/DMSO (95/5) at room temperature (≈ 22°C). The reported data points are the result of a single kinetic measurement realized on a solution from the PSS_{370}: 0 to 3930 min (step = 15 min).

$$k_{295} = 1.7 \times 10^{-5}\ min^{-1}$$
$$t_{1/2} = 41991.1\ min \cong 29.1\ days$$

Half-life of compound Z-3 in H_2O

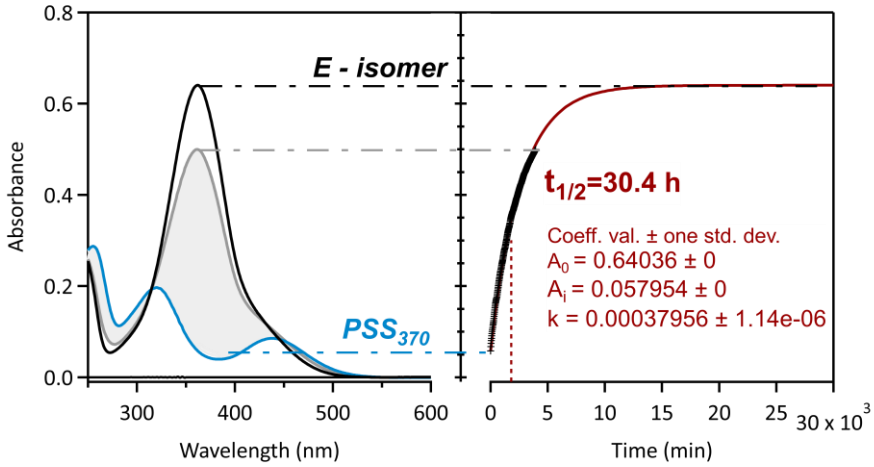

Figure S11: UV-Vis absorption spectra (left) and thermal return monitoring (right) of *Z*-**3** at 362 nm in H_2O at room temperature (≈ 22°C). The reported data points are the result of a single kinetic measurement realized on a solution from the PSS_{370}: 0 to 3940 min (step = 20 min).

$$k_{295} = 3.8 \times 10^{-4}\ min^{-1}$$
$$t_{1/2} = 1826.2\ min \cong 30.4\ h$$

Half-life of compound Z-3 in Tris buffer/DMSO (9/1)

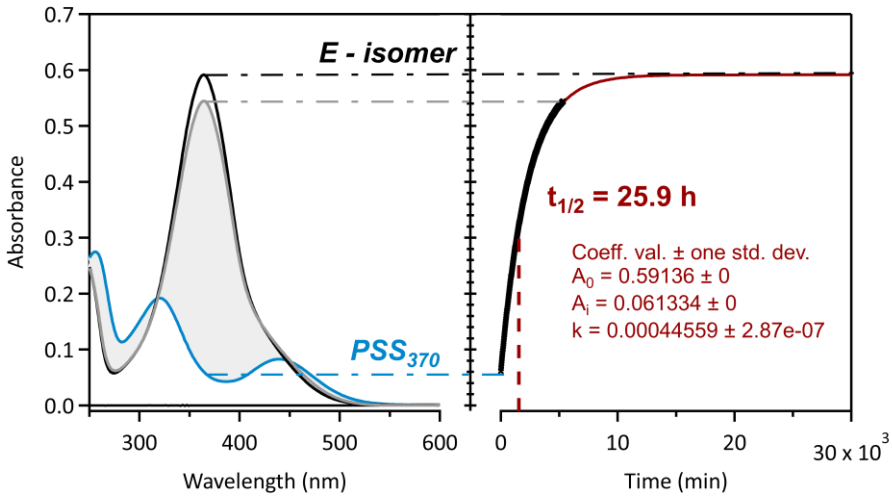

Figure S12: UV-Vis absorption spectra (left) and thermal return monitoring (right) of *Z*-**3** at 364 nm in Tris buffer/DMSO (9/1) at room temperature (≈ 22°C). The reported data points are the result of a single kinetic measurement realized on a solution from the PSS_{370}: 0 to 5340 min (step = 20 min).

$$k_{295} = 4.5 \times 10^{-4}\ min^{-1}$$
$$t_{1/2} = 1555.6\ min \cong 25.9\ h$$

Half-life of compound Z-4 in Tris buffer/DMSO (9/1)

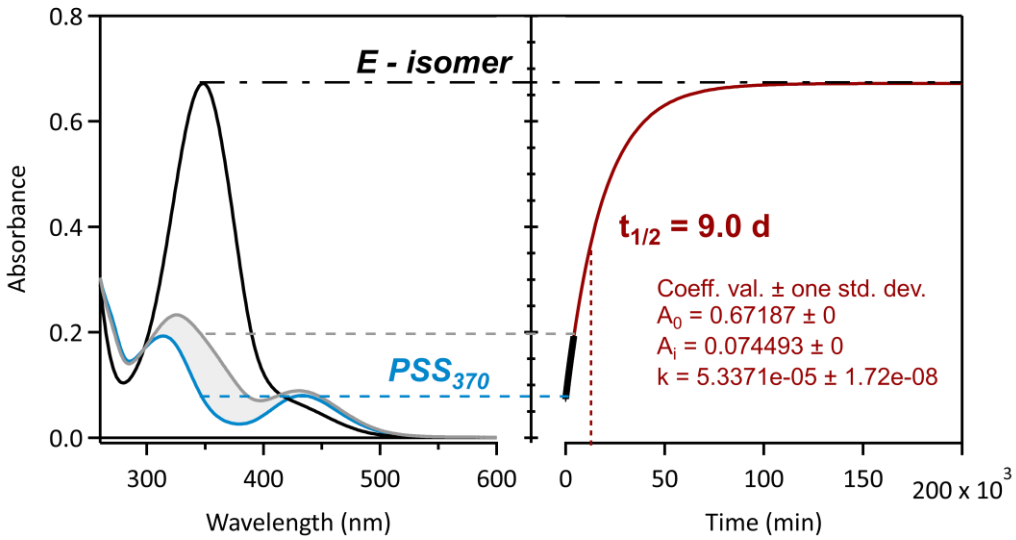

Figure S13: UV-Vis absorption spectra (left) and thermal return monitoring (right) of *Z*-**4** at 348 nm in Tris buffer/DMSO (9/1) at room temperature (≈ 22°C). The reported data points are the result of a single kinetic measurement realized on a solution from the PSS_{370}: 0 to 4095 min (step = 15 min).

$$k_{295} = 5.3 \times 10^{-5}\ min^{-1}$$
$$t_{1/2} = 12987.6\ min \cong 9.0\ days$$

Half-life of compound Z-5 in Tris buffer/DMSO (9/1)

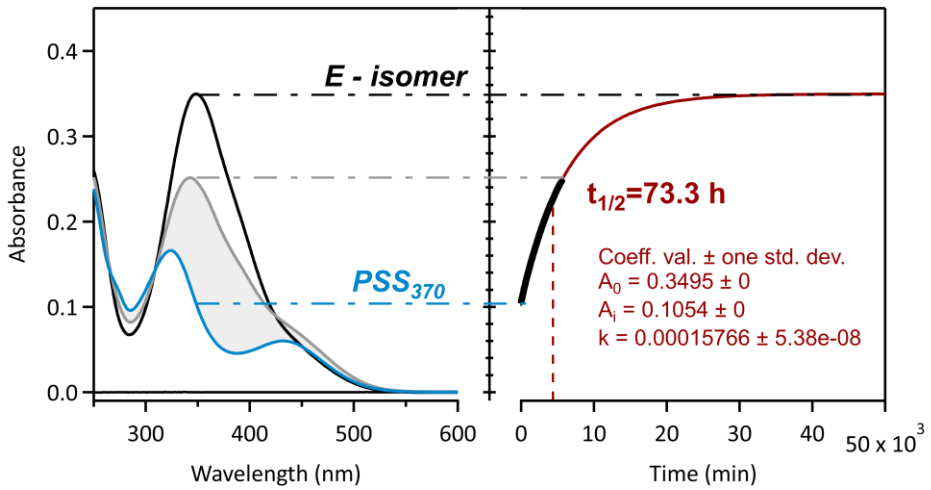

Figure S14: UV-Vis absorption spectra (left) and thermal return monitoring (right) of *Z*-**5** at 348 nm in Tris buffer/DMSO (9/1) at room temperature (≈ 22°C). The reported data points are the result of a single kinetic measurement realized on a solution from the PSS_{370}: 0 to 5595 min (step = 15 min).

$$k_{295} = 1.6 \times 10^{-4}\ min^{-1}$$

$$t_{1/2} = 4396.5\ min \cong 73.3\ h$$

2.3. General procedure for the fatigue resistance measurements

Starting from a solution of compound containing 100% of the *E*-isomer, the solution was irradiated sequentially at 370 nm and at 485 nm or 438 nm. The absorbance was measured before and after each illumination realized with constant optical length distance. The sequence, which constitutes a cycle, was repeated for a minimum of 10 times.

Fatigue resistance of the compound 2

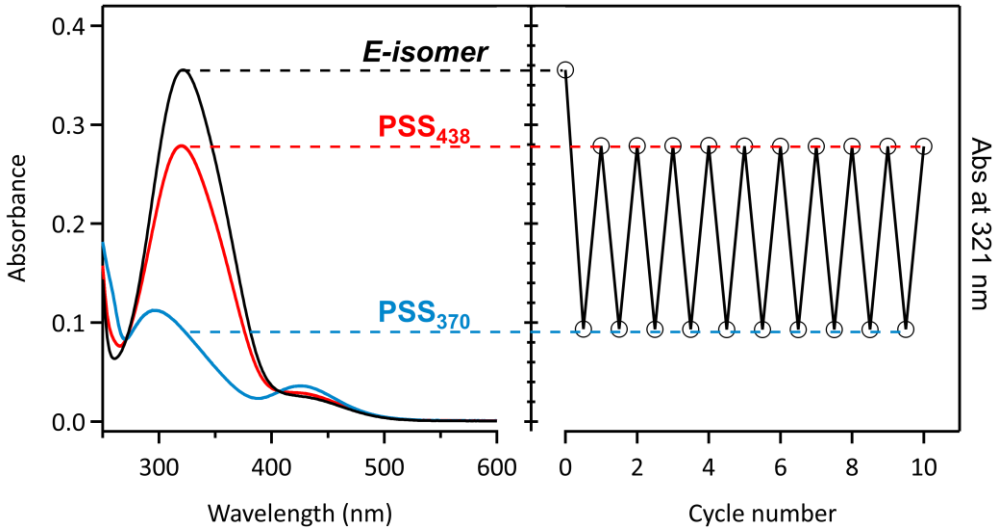

Figure S15: Left: absorption spectra of *E*-**2** (black line), PSS_{370} (blue line), PSS_{438} (red line) in Tris buffer/ DMSO (9/1); Right: Fatigue resistance followed by the absorption band at 321 nm under alternate 370 nm/438 nm irradiation cycles in Tris buffer/DMSO (9/1). Irradiation conditions: 40 s at P_{370} = 14.1 mW cm^{-2} and 180 s at P_{438} = 10.0 mW cm^{-2}.

Fatigue resistance of the compound 3

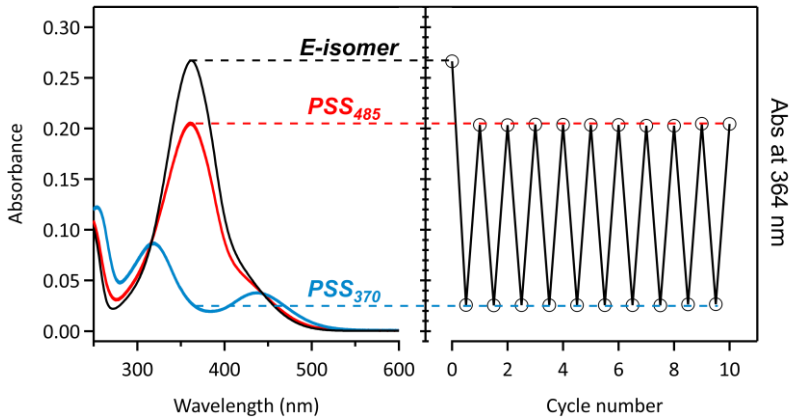

Figure S16: Left: absorption spectra of *E*-**3** (black line), PSS_{370} (blue line), PSS_{485} (red line) in Tris buffer/DMSO (9/1); Right: Fatigue resistance followed by the absorption band at 364 nm under alternate 370 nm/485 nm irradiation cycles in Tris buffer/DMSO (9/1). Irradiation conditions: 30 s at P_{370} = 12.8 mW cm^{-2} and 480 s at P_{485} = 1.5 mW cm^{-2}.

Fatigue resistance of the compound 4

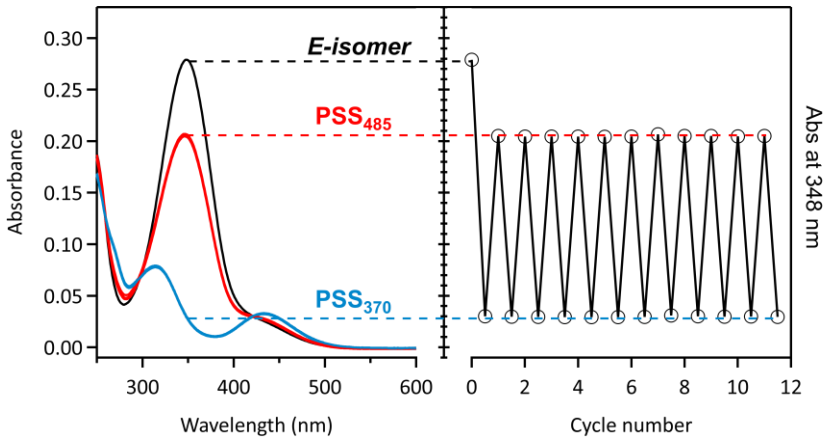

Figure S17: Left: absorption spectra of *E*-**4** (black line), PSS_{370} (blue line), PSS_{485} (red line) in Tris buffer: DMSO (9:1); Right: Fatigue resistance followed by the absorption band at 348 nm under alternate 370 nm/485 nm irradiation cycles in Tris buffer/DMSO (9/1). Irradiation conditions: 40 s at P_{370} = 14.1 mW cm^{-2} and 720 s at P_{485} = 1.6 mW cm^{-2}.

Fatigue resistance of the compound 5

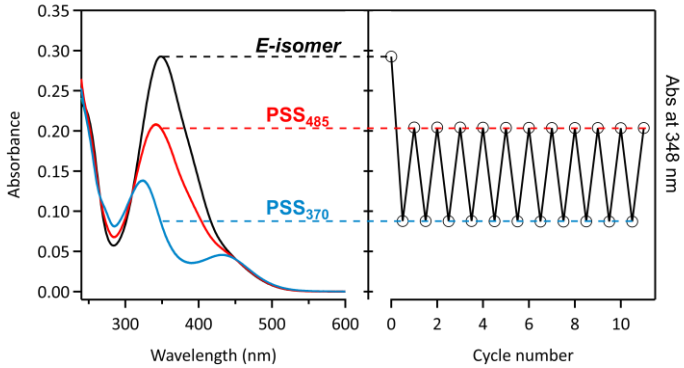

Figure S18: Left: absorption spectra of *E*-**5** (black line), PSS_{365} (blue line), PSS_{485} (red line) in Tris buffer/DMSO (9/1); Right: Fatigue resistance followed by the absorption band at 348 nm under alternate 370 nm/485 nm irradiation cycles in Tris buffer/DMSO (9/1). Irradiation conditions: 30 s at P_{370} = 14.1 mW cm^{-2} and 540 s at P_{485} = 1.6 mW cm^{-2}.

2.4. General procedure for the determination of the photoconvertion yields by absorption and ^{1}H NMR

A solution of *E*-isomer was extemporaneously prepared in D_2O or a mixture solvent D_2O/DMSO-d_6 9/1 with the maximum absorbance was close to 1. The deuterated solution was monitored by absorption and ^{1}H NMR before and after irradiation. It is worth noting that the absorbance was recorded first and then a small amount of the solution was taken for ^{1}H NMR monitoring. The sequence was repeated after irradiating the solution to the photostationary state (PSS), and ^{1}H NMR spectra were recorded with a relaxation delay of 0.5 s and 512 scans, in order to have reasonable acquisition time to prevent the impact of thermal return. Then, the corresponding photoconversion yield (CY) was calculated after integrating the pic area according to the following equation,

$$CY_i = \frac{A_E}{A_E + A_Z}$$

With,
CY_i, represents the conversion yield for a given state (i) of the solution,
A_E, represents the area taken under the pic of *E*-isomer signal,
A_Z, represents the area taken under the pic of *Z*-isomer signal.

Study of photoisomerization for compound 1

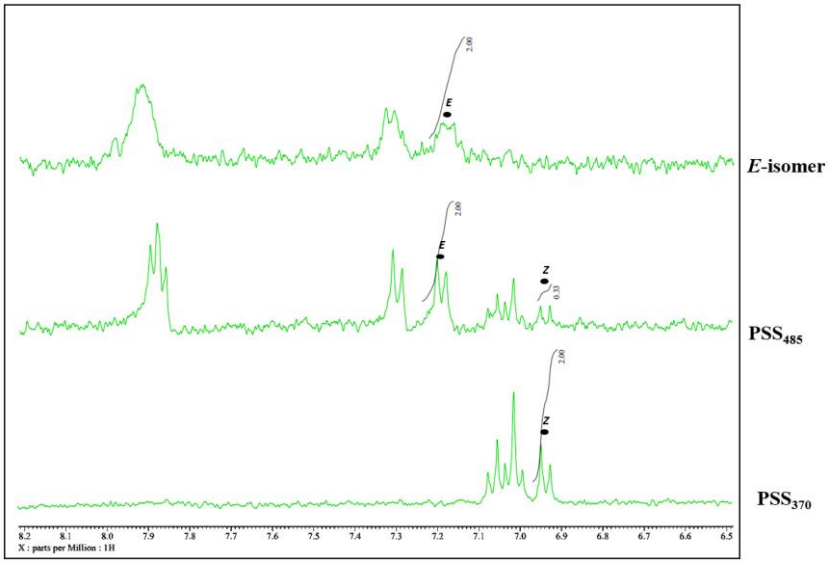

Figure S19: ^{1}H NMR spectra of *E*-**1**, PSS_{370} and PSS_{485} azobenzene region in D_2O. The integral values taken for the determination of the photoconversion yields.

Study of photoisomerization for compound 2

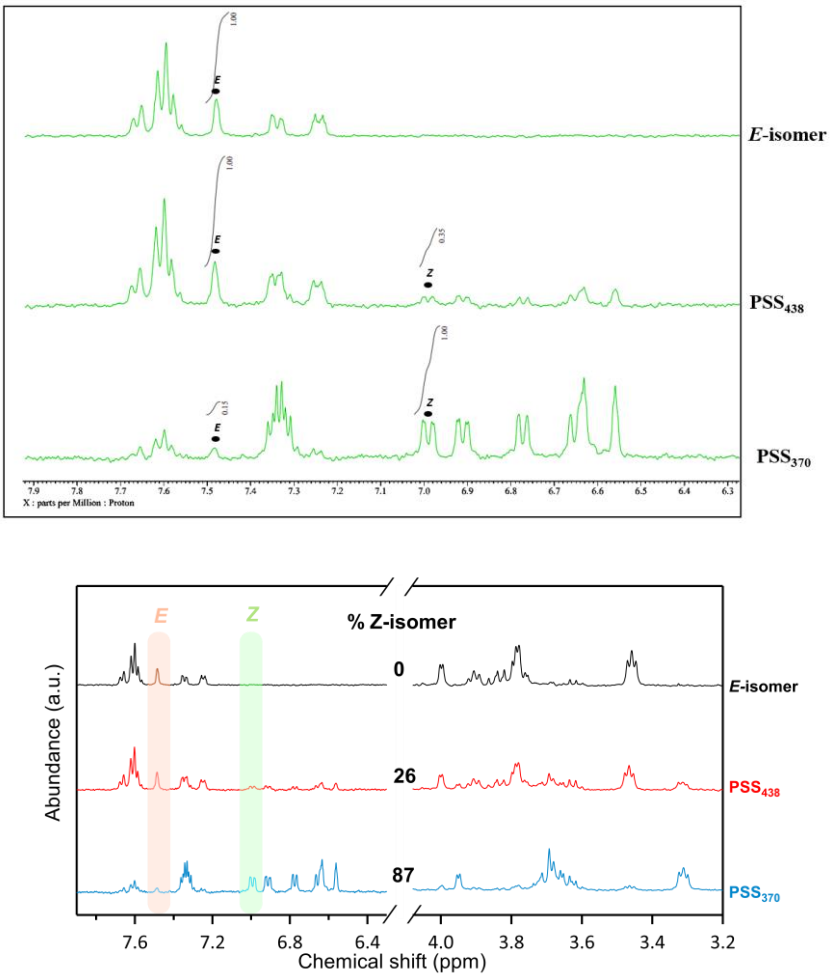

Figure S20: Partial ^{1}H NMR spectra of *E*-**2** (black line), PSS_{370} (blue line) and PSS_{438} (red line) in D_2O/DMSO-d_6 (9/1). Top graph: the region of azobenzene and the integral values taken for the determination of the photoconversion yields.

Study of photoisomerization for compound 3

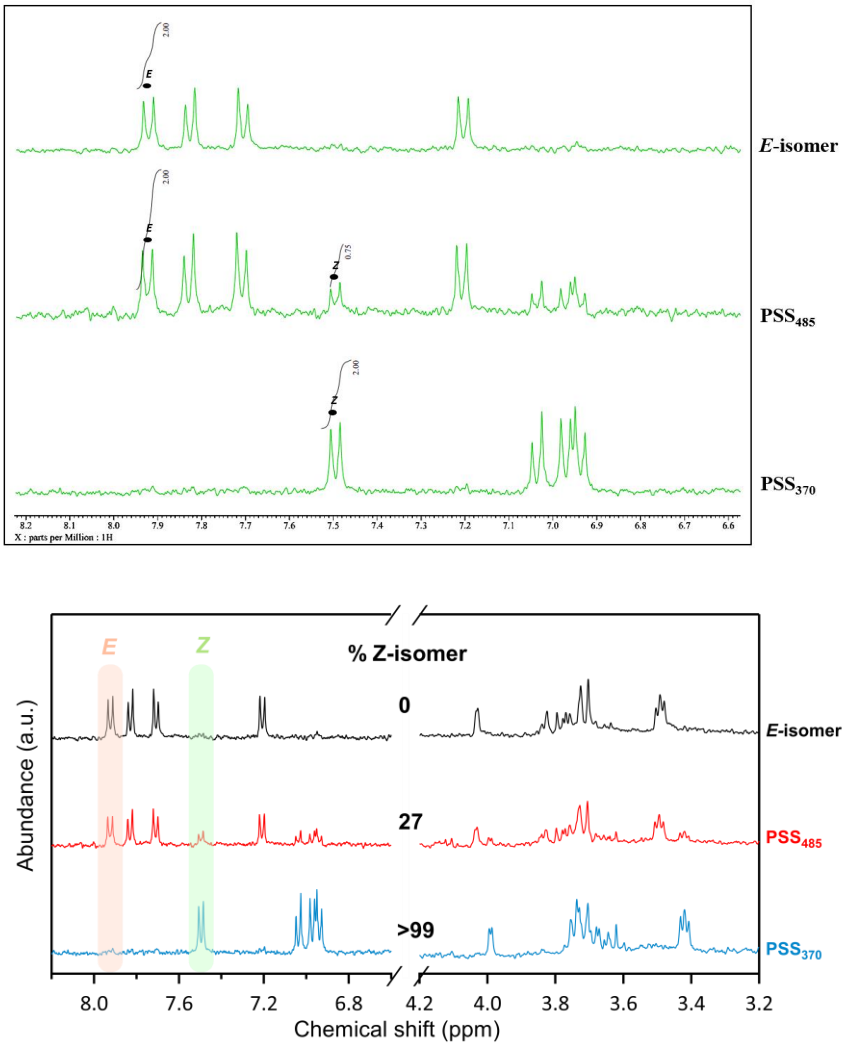

Figure S21: Partial ^{1}H NMR spectra of *E*-**3** (black line), PSS_{370} (blue line) and PSS_{485} (red line) in D_2O. Top graph: the region of azobenzene and the integral values taken for the determination of the photoconversion yields.

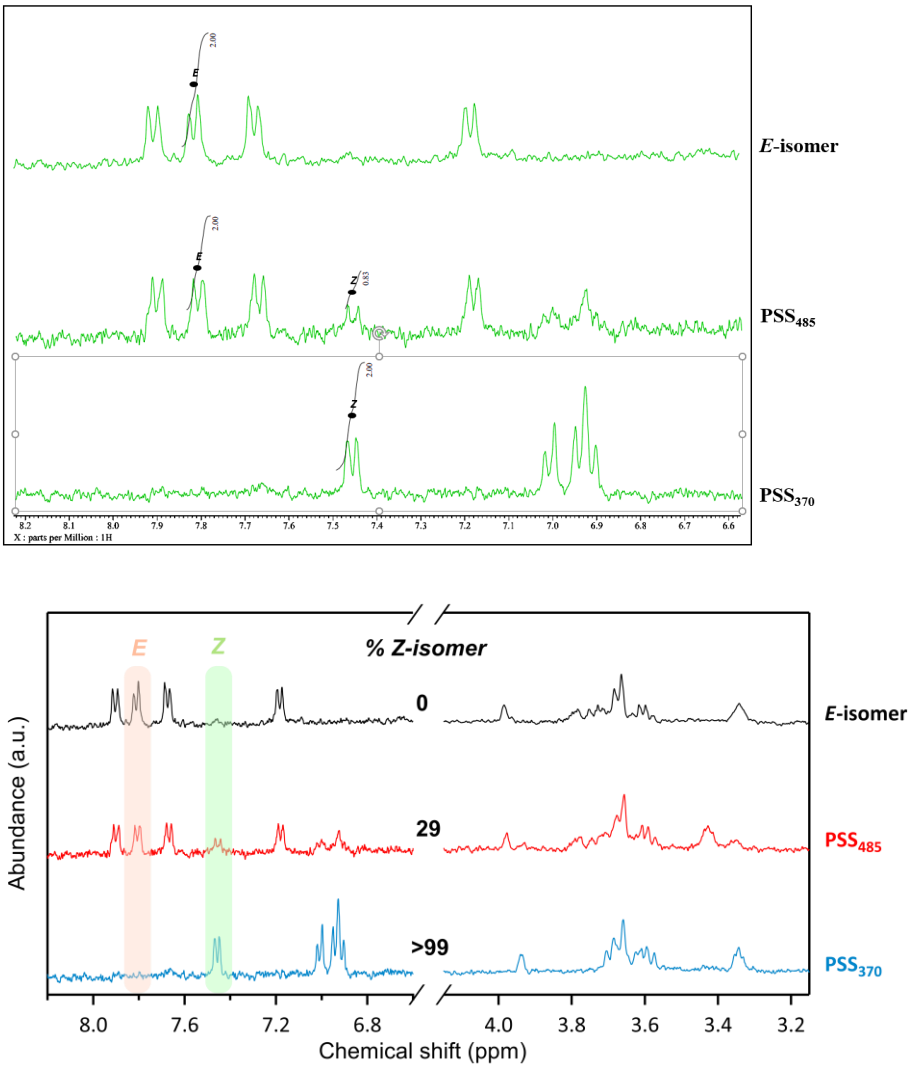

Figure S22: Partial ^{1}H NMR spectra of *E*-**3** (black line), PSS_{370} (blue line) and PSS_{485} (red line) in D_2O/DMSO-d_6 (9/1). Top graph: the region of azobenzene and the integral values taken for the determination of the photoconversion yields.

Study of photoisomerization for compound 4

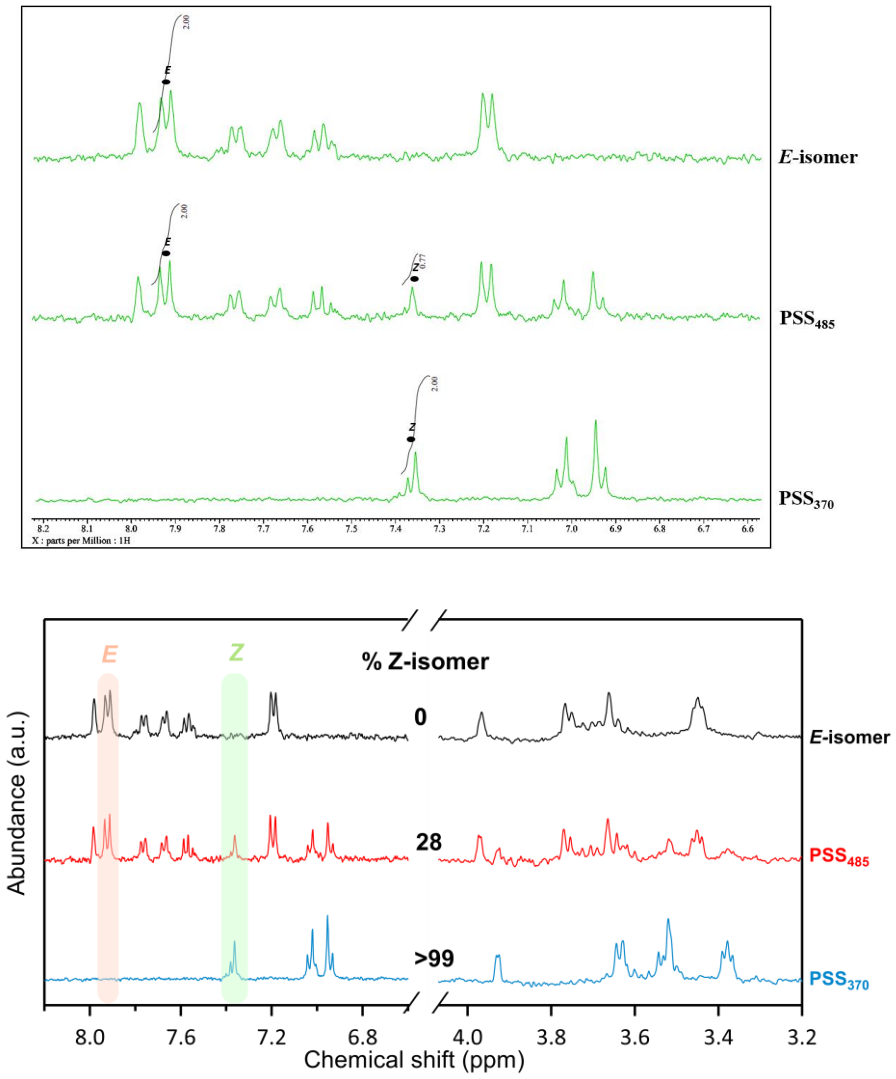

Figure S23: Partial ^{1}H NMR spectra of *E*-**4** (black line), PSS_{370} (blue line) and PSS_{485} (red line) in D_2O/DMSO-d_6 (9/1). Top graph: the region of azobenzene and the integral values taken for the determination of the photoconversion yields.

Study of photoisomerization for compound 5

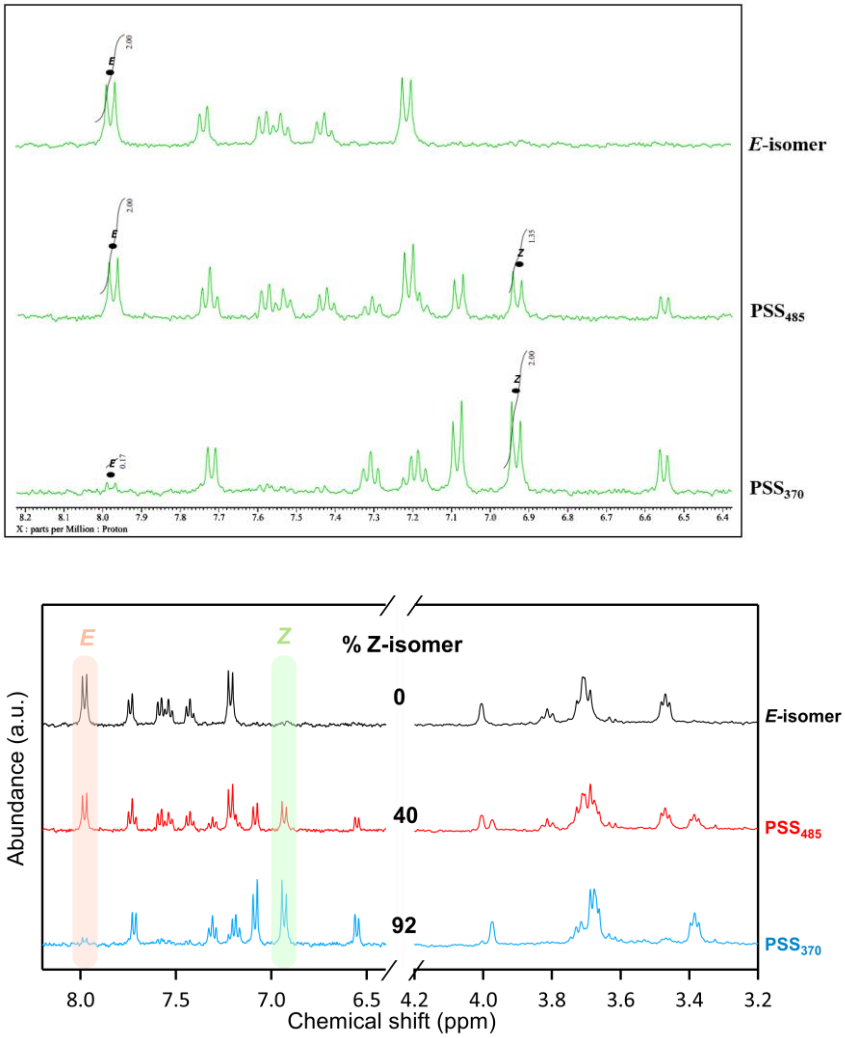

Figure S24: Partial ^{1}H NMR spectra of *E*-**5** (black line), PSS_{370} (blue line) and PSS_{485} (red line) in D_2O/DMSO-d_6 (9/1). Top graph: the region of azobenzene and the integral values taken for the determination of the photoconversion yields.

3. Concentration of ligands determined by spectroscopy

In previous studies on spectroscopic properties, we measured the molar absorption coefficient (Ɛ) of pure *E*-isomer, and the maximum photoconversion yield of the ligands from *E*-isomer to *Z*-isomer when they reached the photostationary state (PSS) after irradiation at 365 nm. The concentration of the ligands was calculated by following formula:

$$c = \frac{A(\lambda)}{\varepsilon(\lambda) l}$$

with

$A(\lambda)$, represents the absorbance at the wavelength λ

$\varepsilon(\lambda)$, represents the molar absorption coefficient at the wavelength λ, in $mol \cdot L^{-1} \cdot cm^{-1}$

l, the distance of the trajectory in the media, in cm

C, the concentration of the substrate in $mol \cdot L^{-1}$

Table S1: The concentration of ligands.

ligand	solvent	Concentration 1 (mM)	Concentration 2 (mM)
E-1	Tris buffer: DMSO (95:5)	2.9	n.d.[c]
Z-1	Tris buffer: DMSO (95:5)	3.0	n.d.
E-2	Tris buffer: DMSO (9:1)	3.0	2.9
Z-2	Tris buffer: DMSO (9:1)	3.0	2.9
E-3	Tris buffer: DMSO (9:1)	2.0	n.d.
Z-3	Tris buffer: DMSO (9:1)	2.0	n.d.
E-4	Tris buffer: DMSO (9:1)	3.0	3.0
Z-4	Tris buffer: DMSO (9:1)	3.0	2.9
E-5	Tris buffer: DMSO (9:1)	3.0	2.9
Z-5	Tris buffer: DMSO (9:1)	3.0	2.9

Concentration 1: The concentration was calculated from weighted mass; Concentration 2: The concentration was calculated by spectroscopy; [c] not determined.

4. ^{1}H and $^{13}C\{^{1}H\}$ NMR Spectra

^{1}H NMR of compound *E*-1 in CD_3OD at 400 MHz

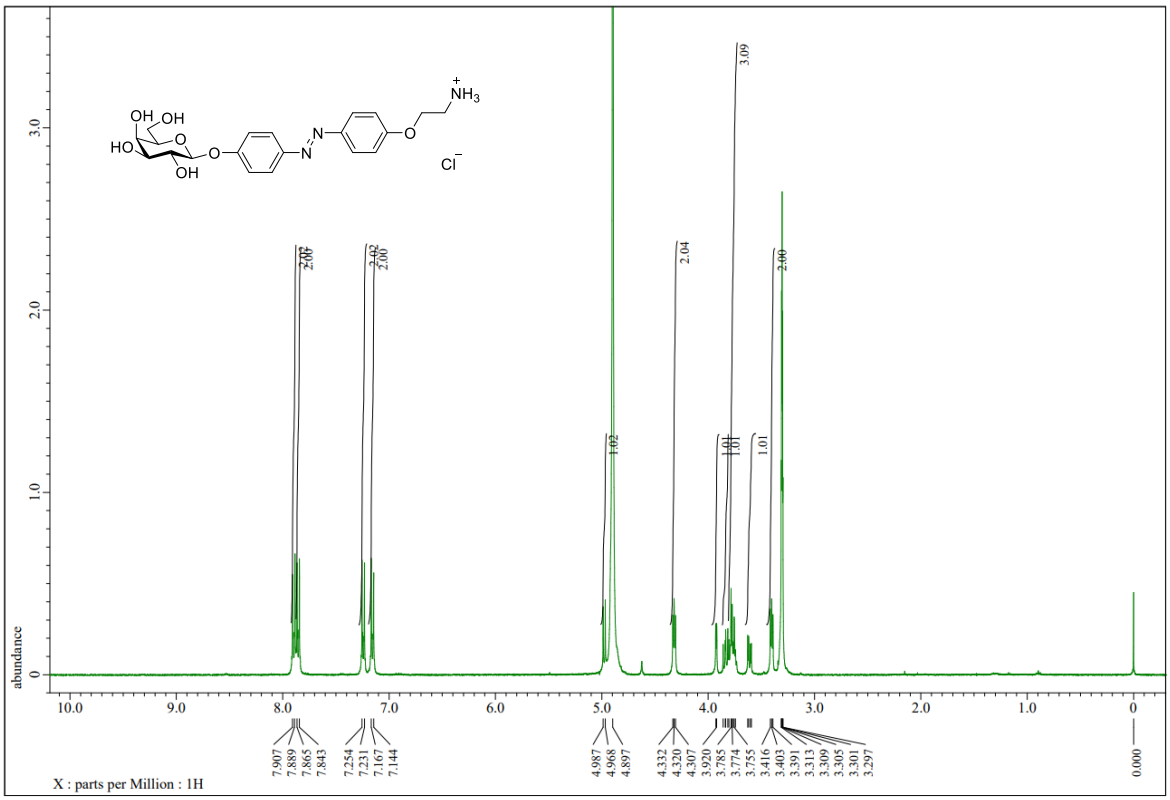

Enlarged ^{1}H NMR of compound *E*-1 in CD_3OD at 400 MHz

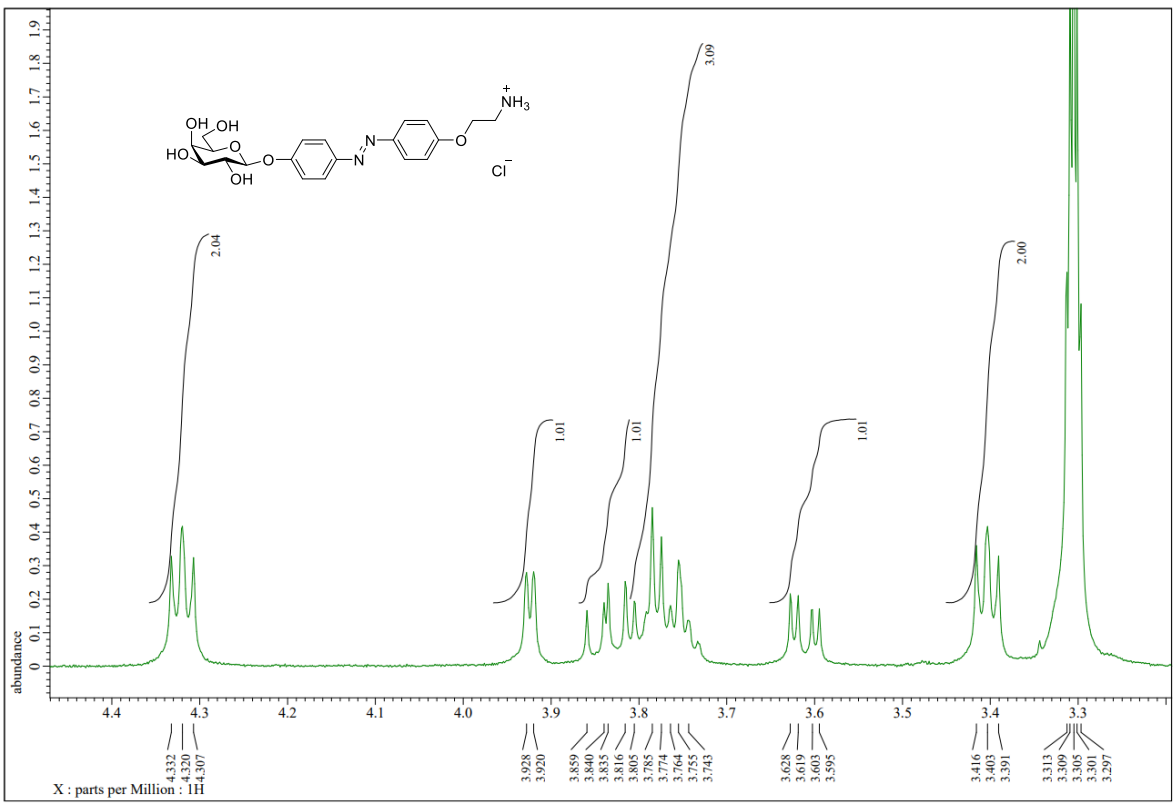

$^{13}C\{^{1}H\}$ NMR (UDEFT) of compound *E*-1 in CD_3OD at 100 MHz

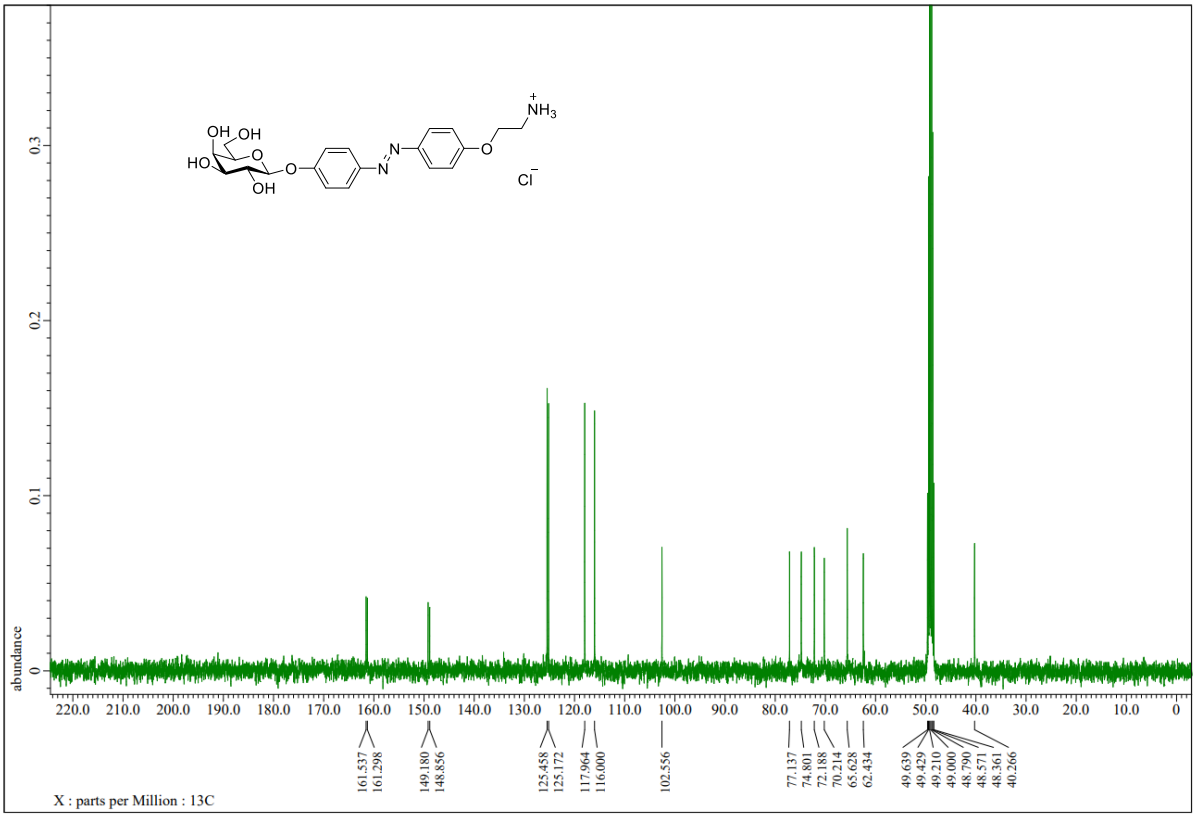

^{1}H NMR of compound *E*-2 in CD_3OD at 400 MHz

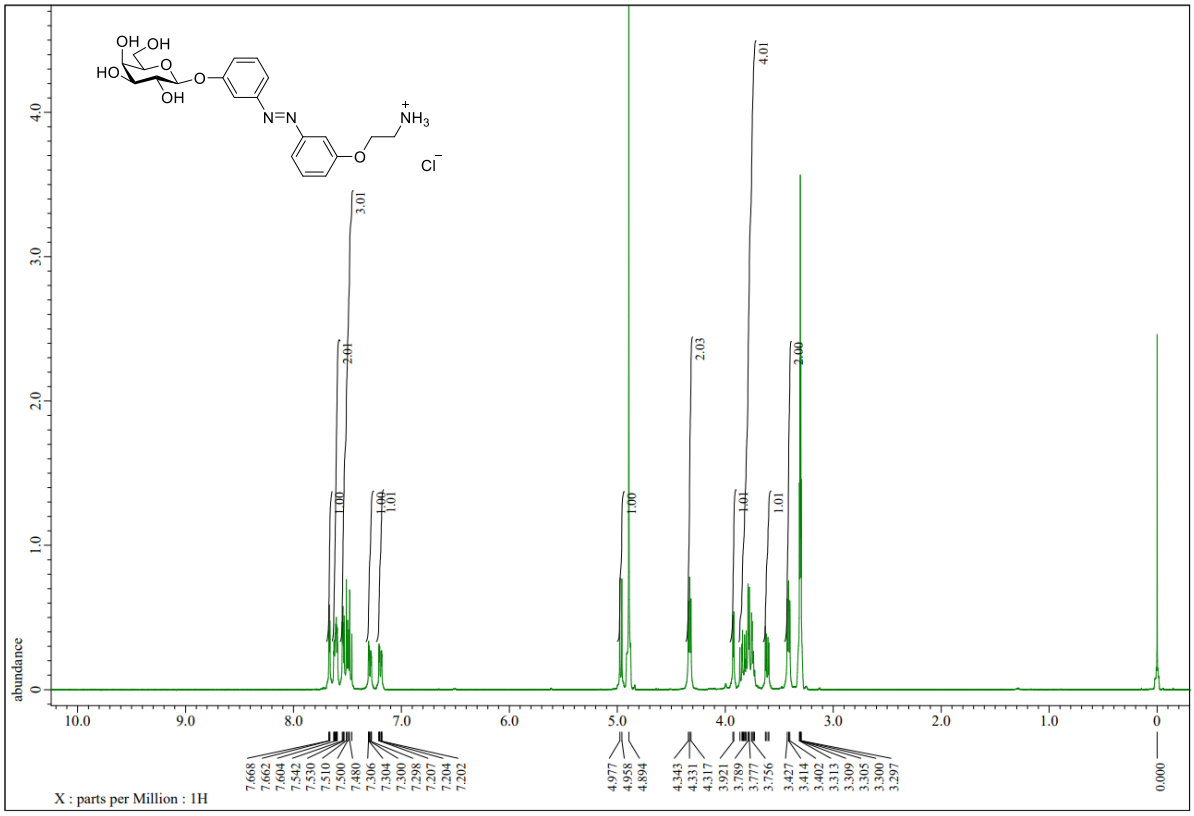

Enlarged ^{1}H NMR of compound *E*-2 in CD_3OD at 400 MHz

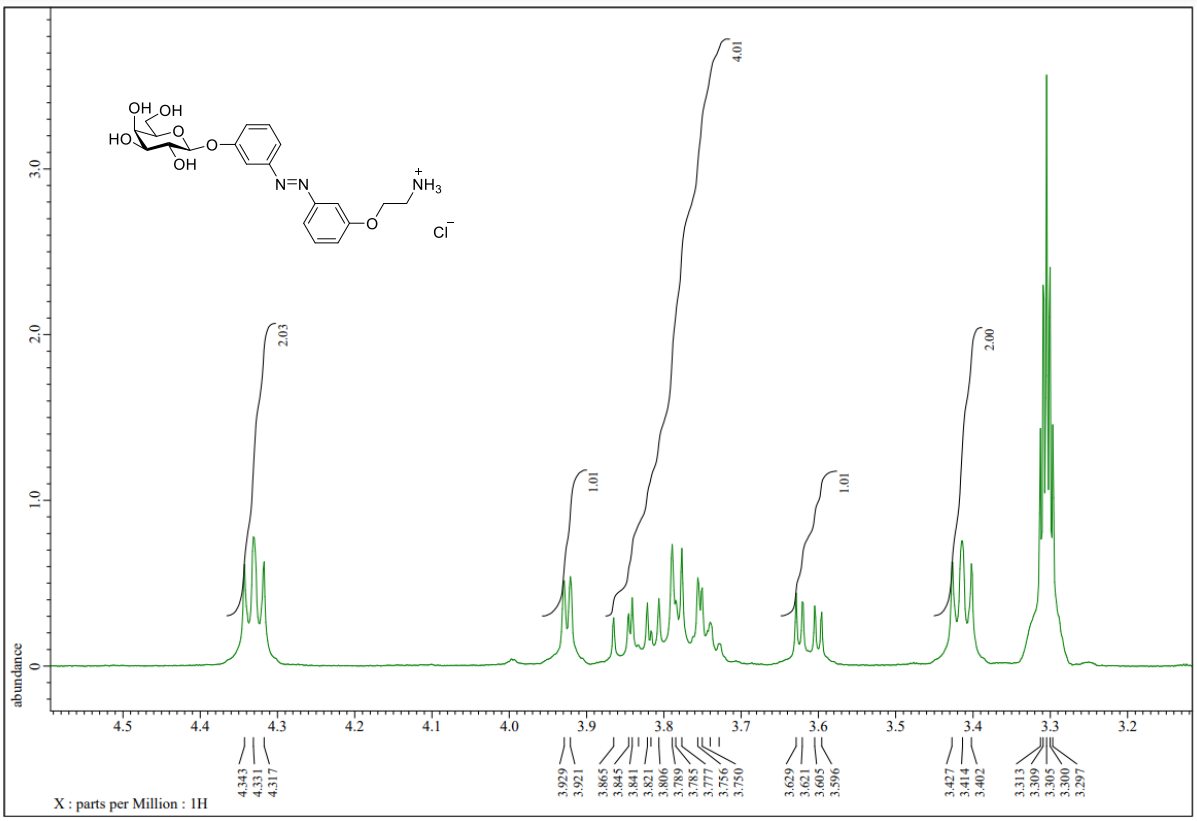

$^{13}C\{^{1}H\}$ NMR of compound *E*-2 in CD_3OD at 100 MHz

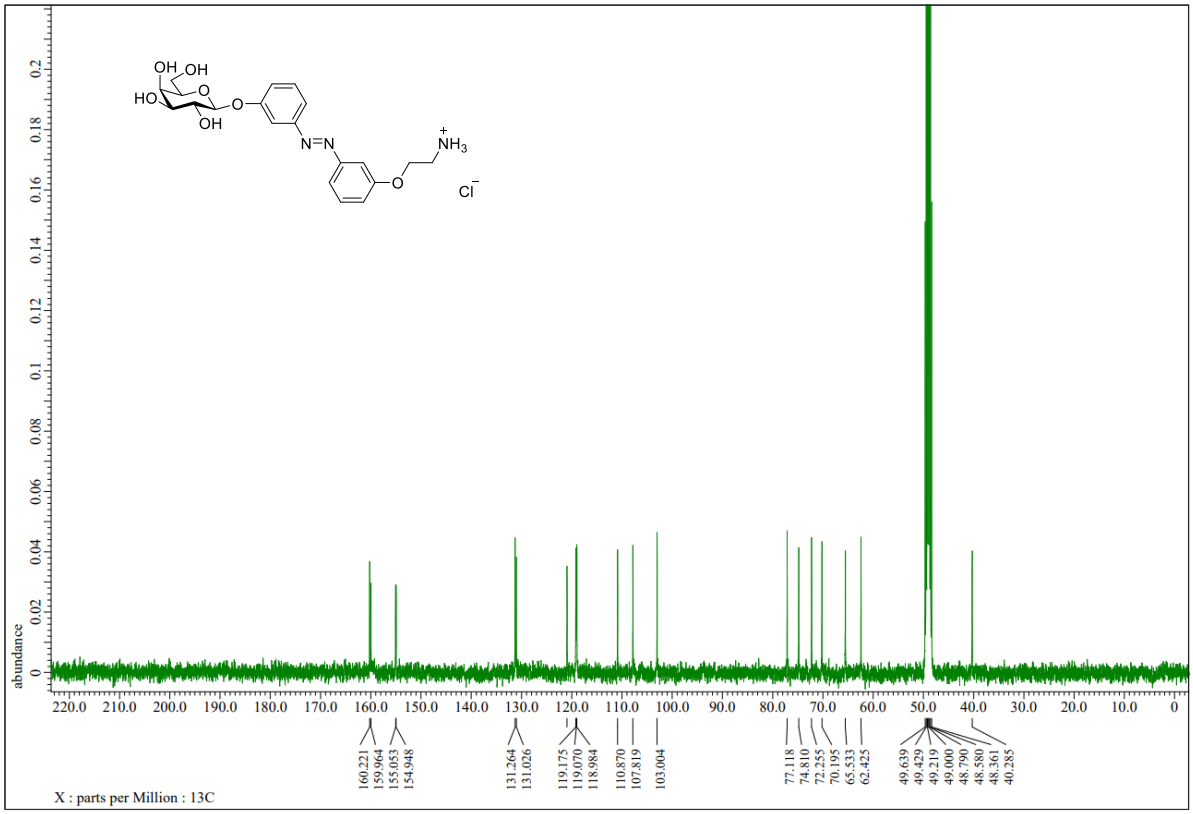

^{1}H NMR of compound *E*-3 in $CDCl_3$ at 400 MHz

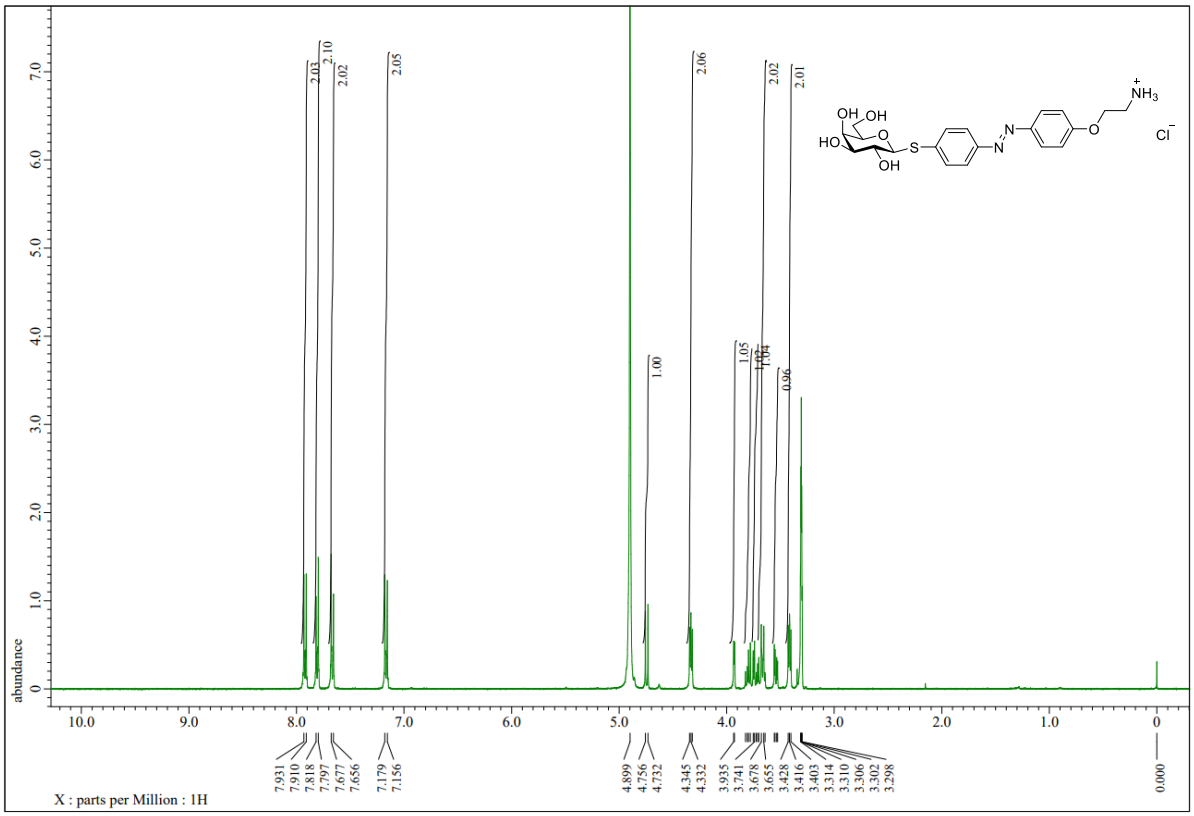

Enlarged ^{1}H NMR of compound *E*-3 in $CDCl_3$ at 400 MHz

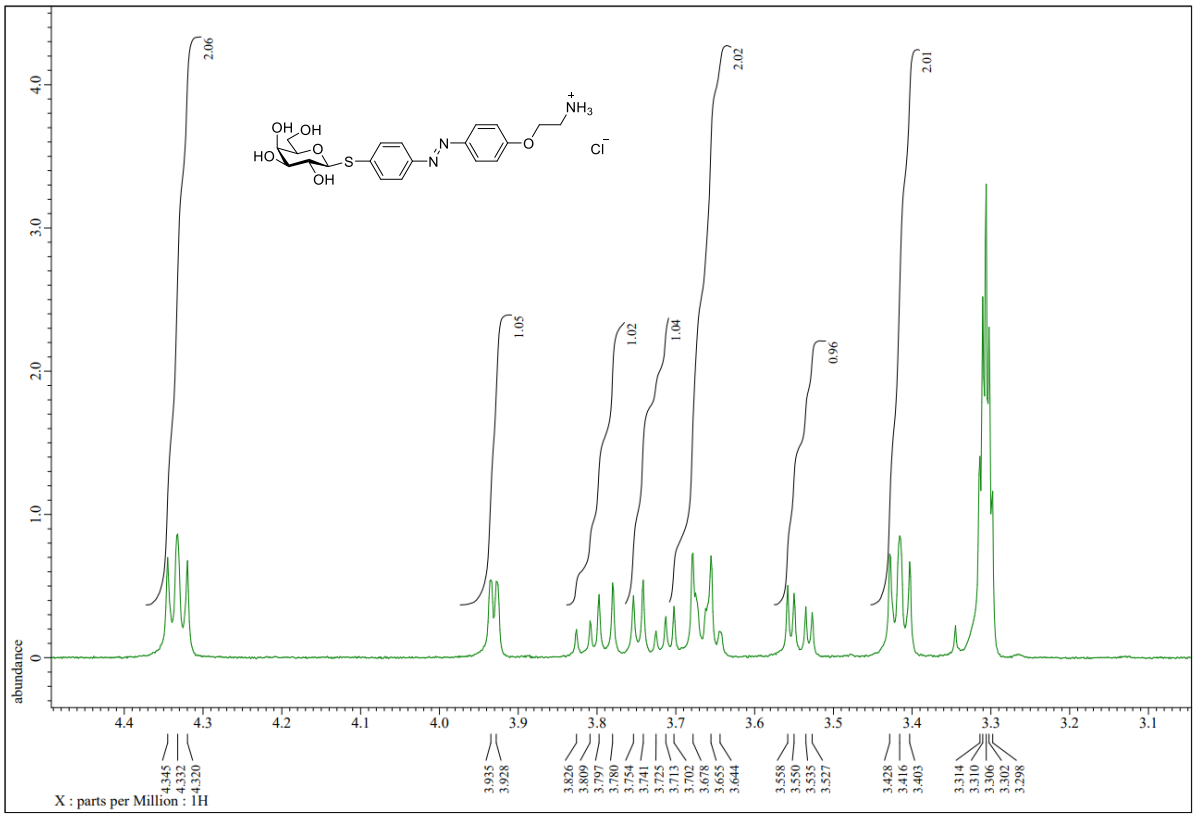

$^{13}C\{^{1}H\}$ NMR (UDEFT) of compound *E*-3 in $CDCl_3$ at 100 MHz

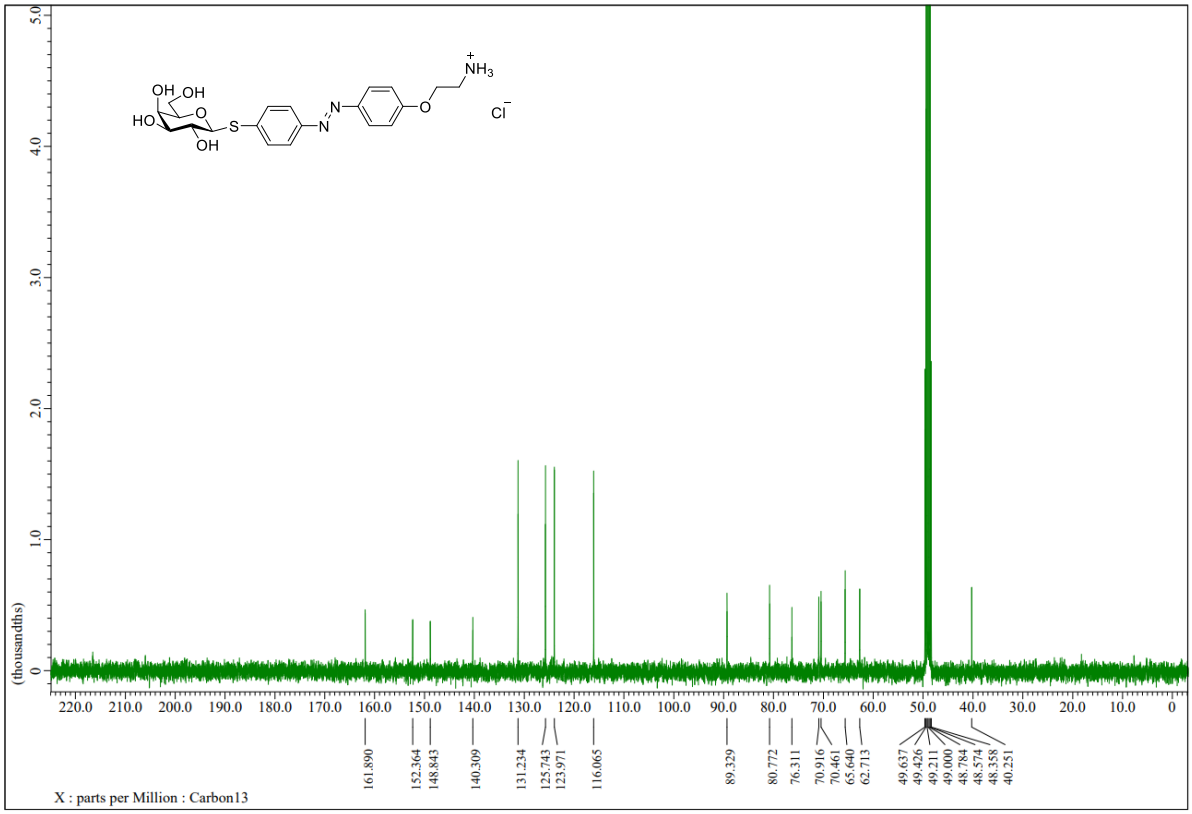

^{1}H NMR of compound *E*-4 in CD_3OD at 400 MHz

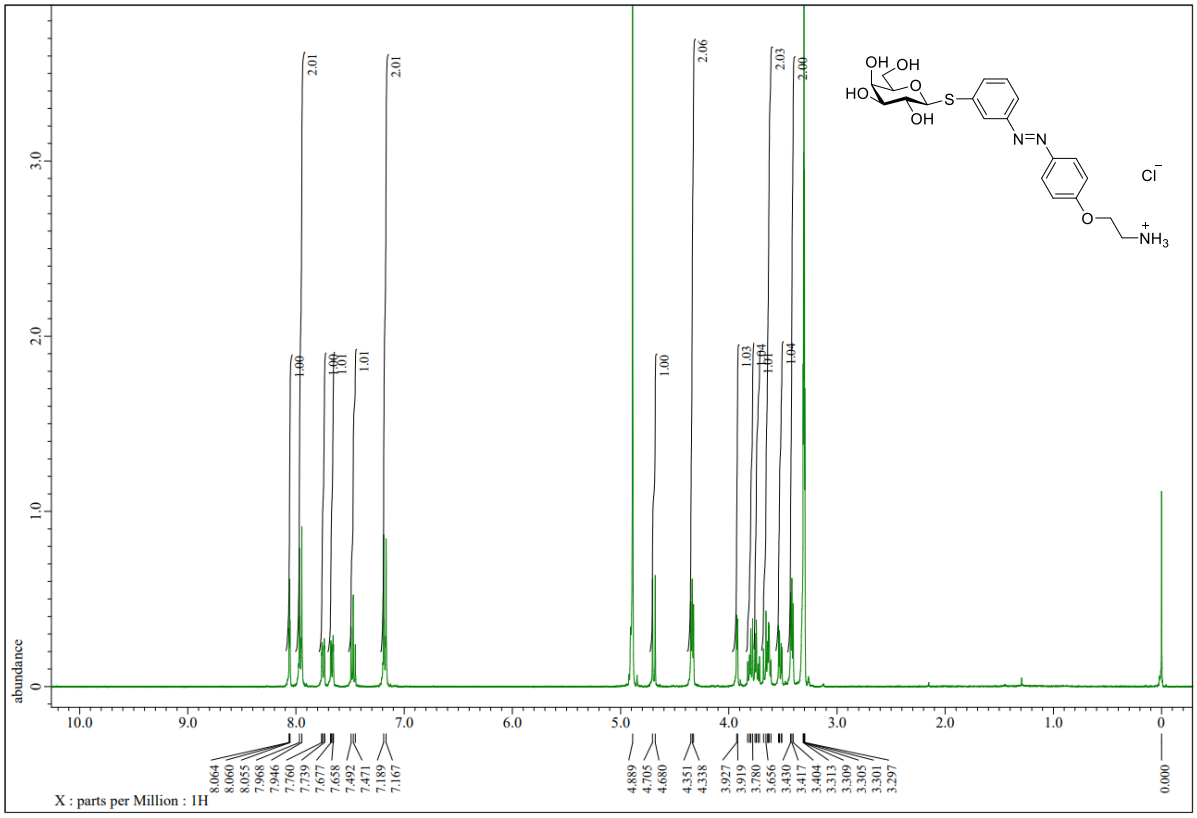

Enlarged ^{1}H NMR of compound *E*-4 in CD_3OD at 400 MHz

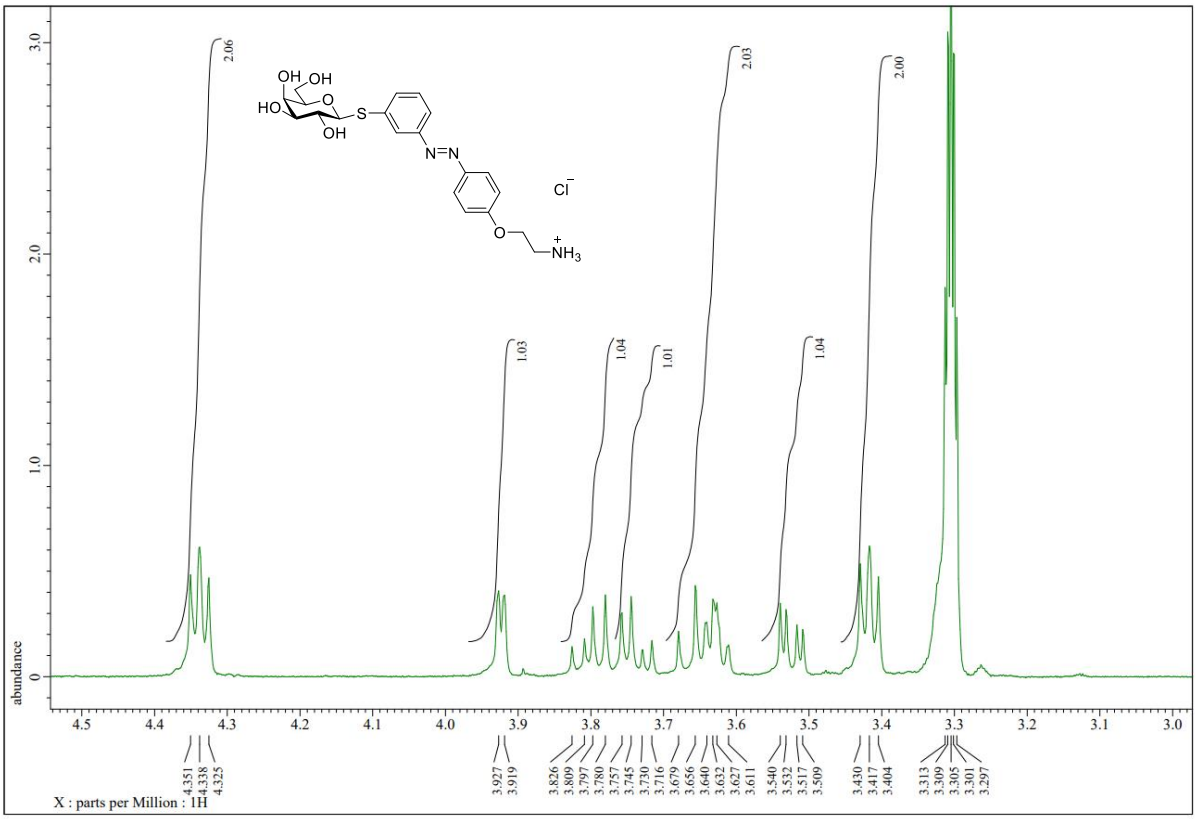

$^{13}C\{^{1}H\}$ NMR of compound *E*-4 in CD_3OD at 100 MHz

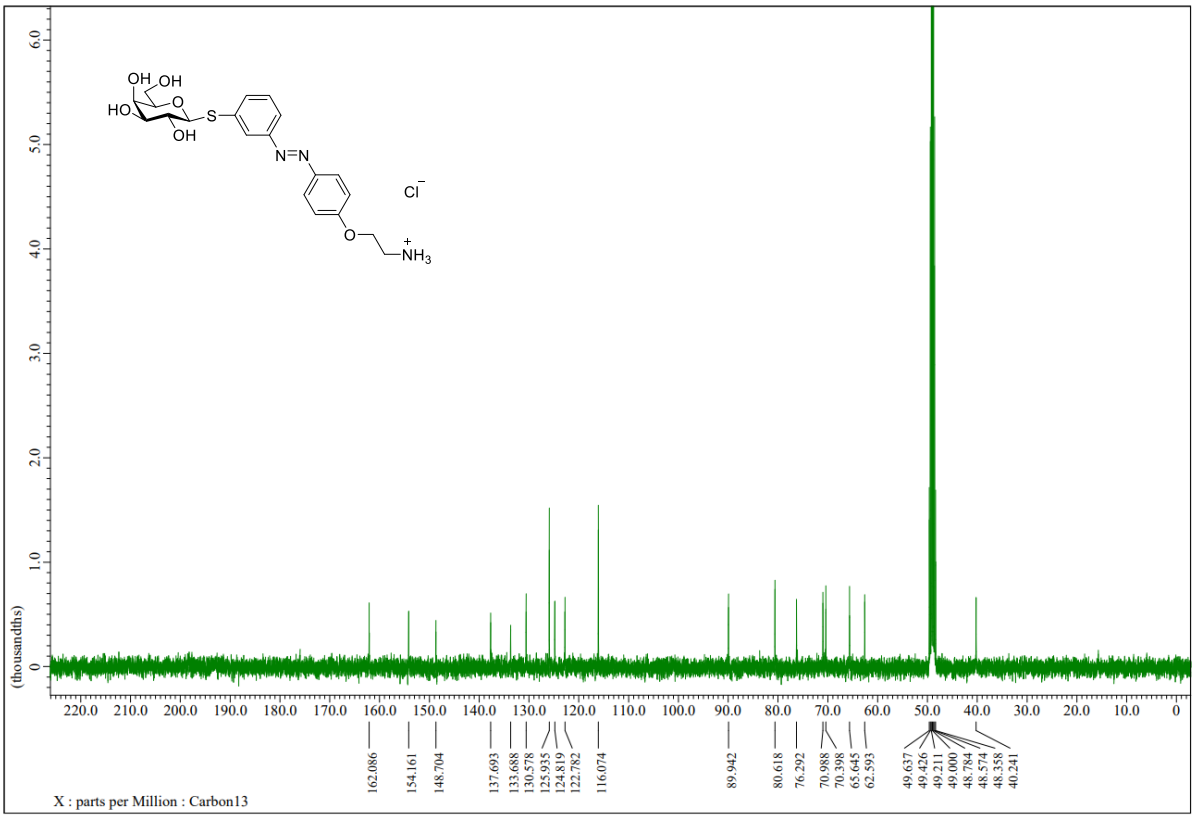

^{1}H NMR of compound *E*-5 in CD_3OD at 400 MHz

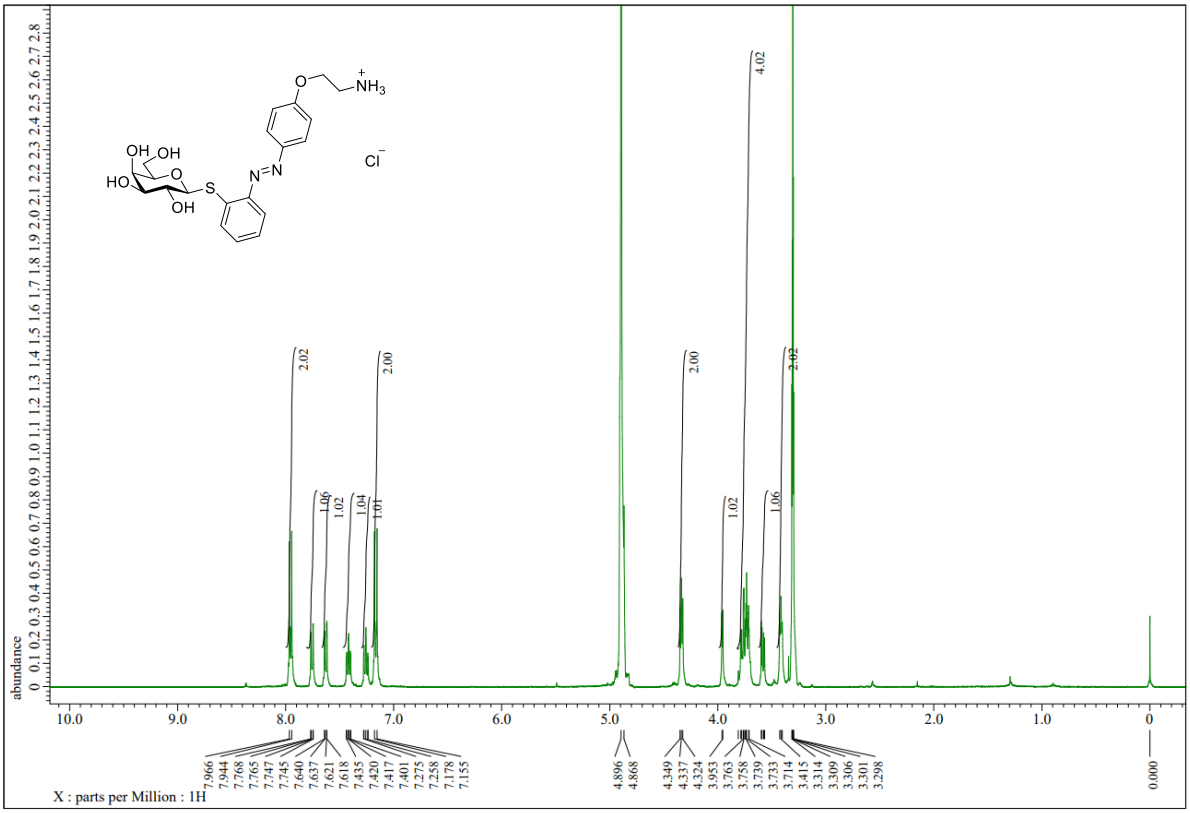

Enlarged ^{1}H NMR of compound *E*-5 in CD_3OD at 400 MHz

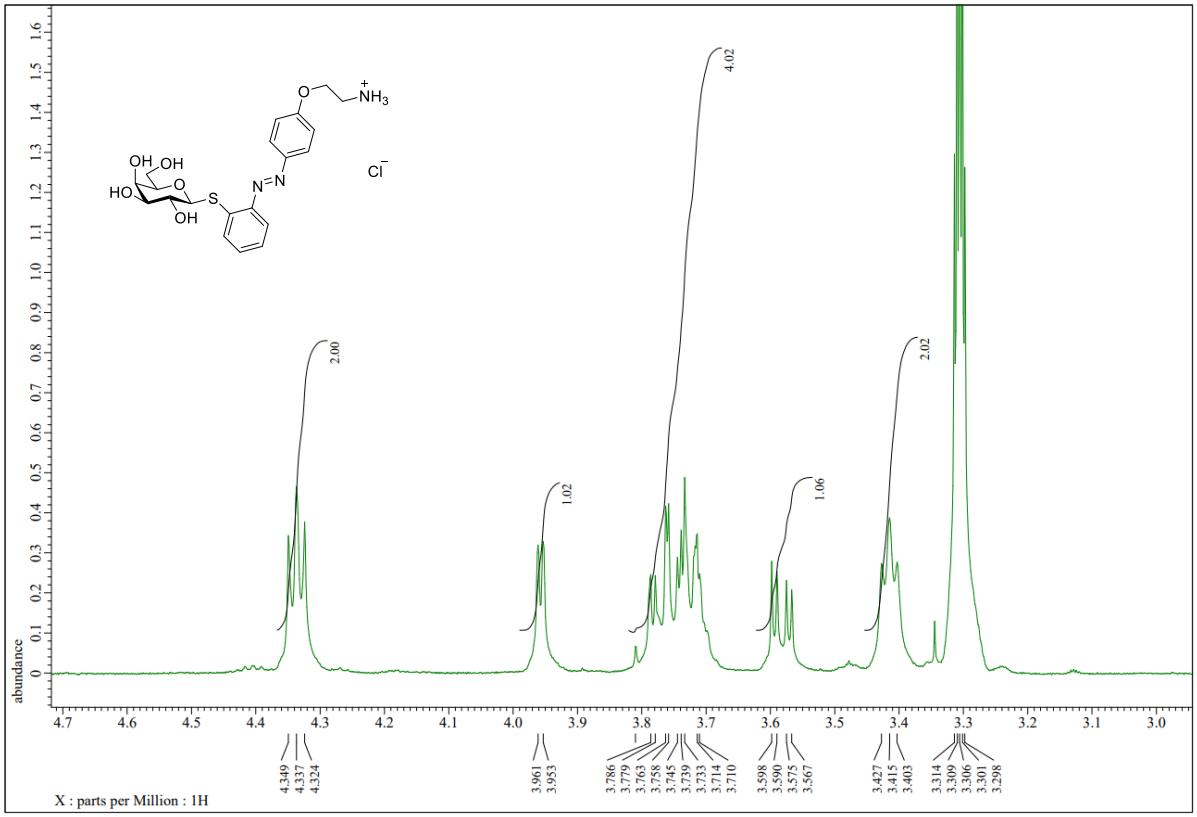

$^{13}C\{^{1}H\}$ NMR of compound *E*-5 in CD_3OD at 100 MHz

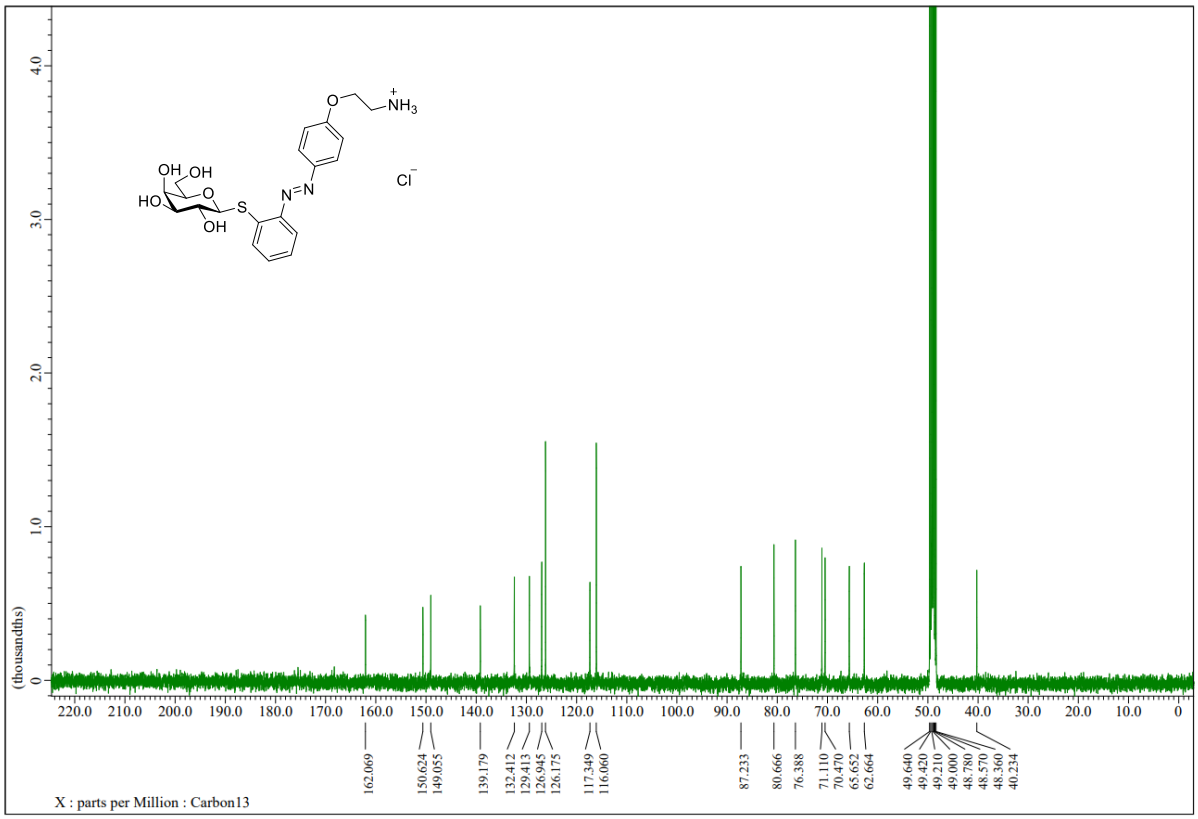

^{1}H NMR of compound *E*-8 in CD_3OD at 400 MHz

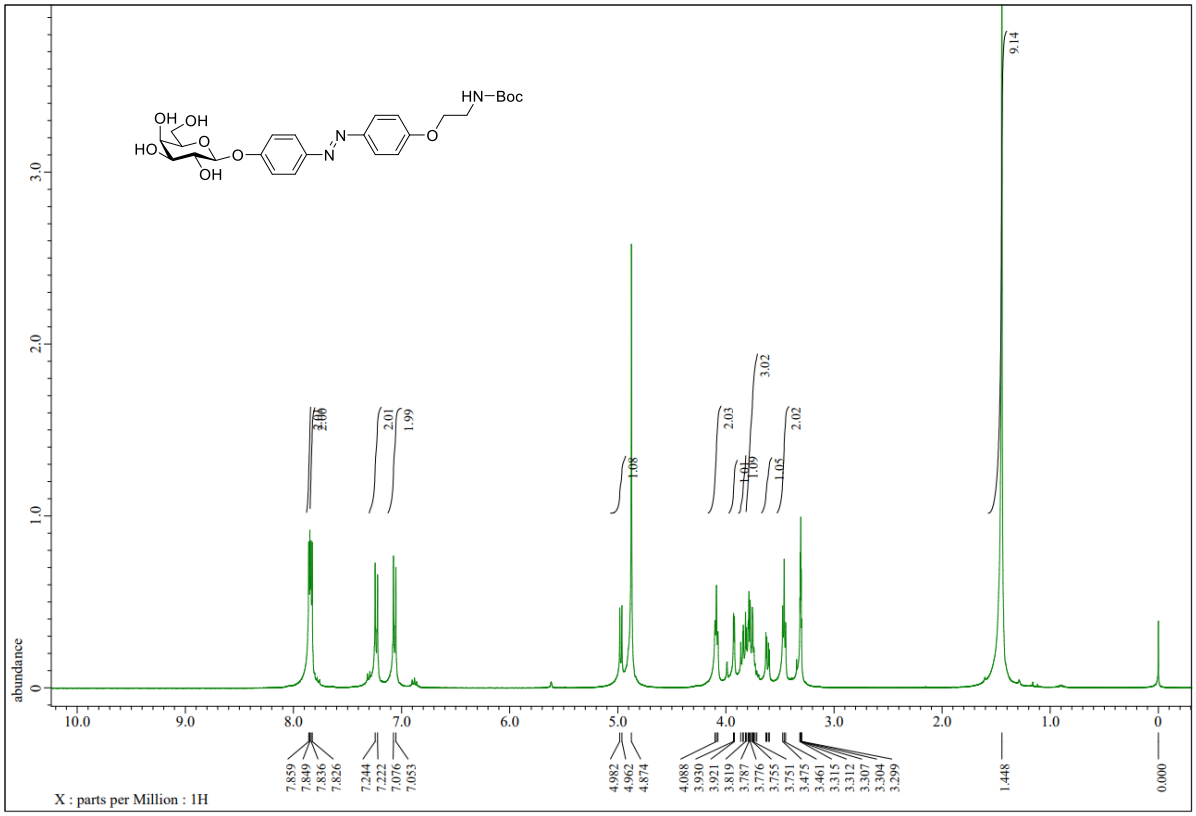

Enlarged ^{1}H NMR of compound *E*-8 in CD_3OD at 400 MHz

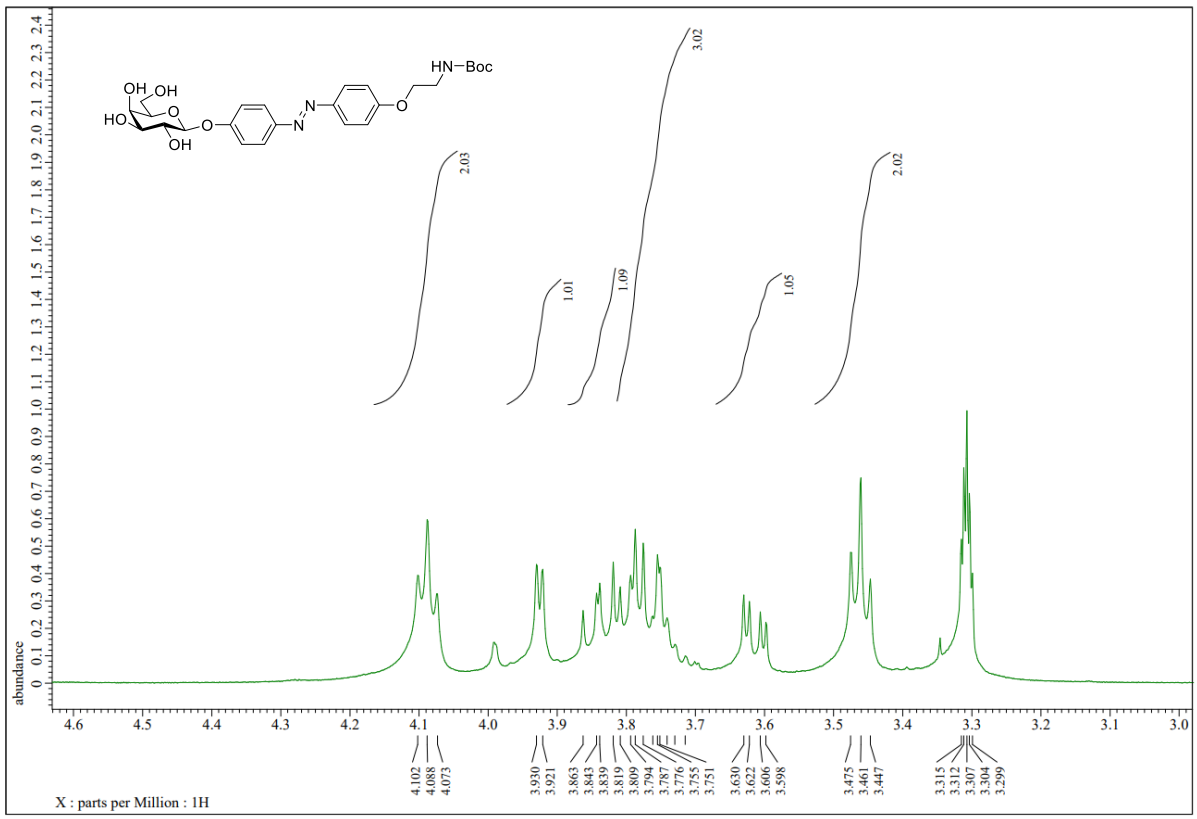

$^{13}C\{^{1}H\}$ NMR (UDEFT) of compound *E*-8 in CD_3OD at 100 MHz

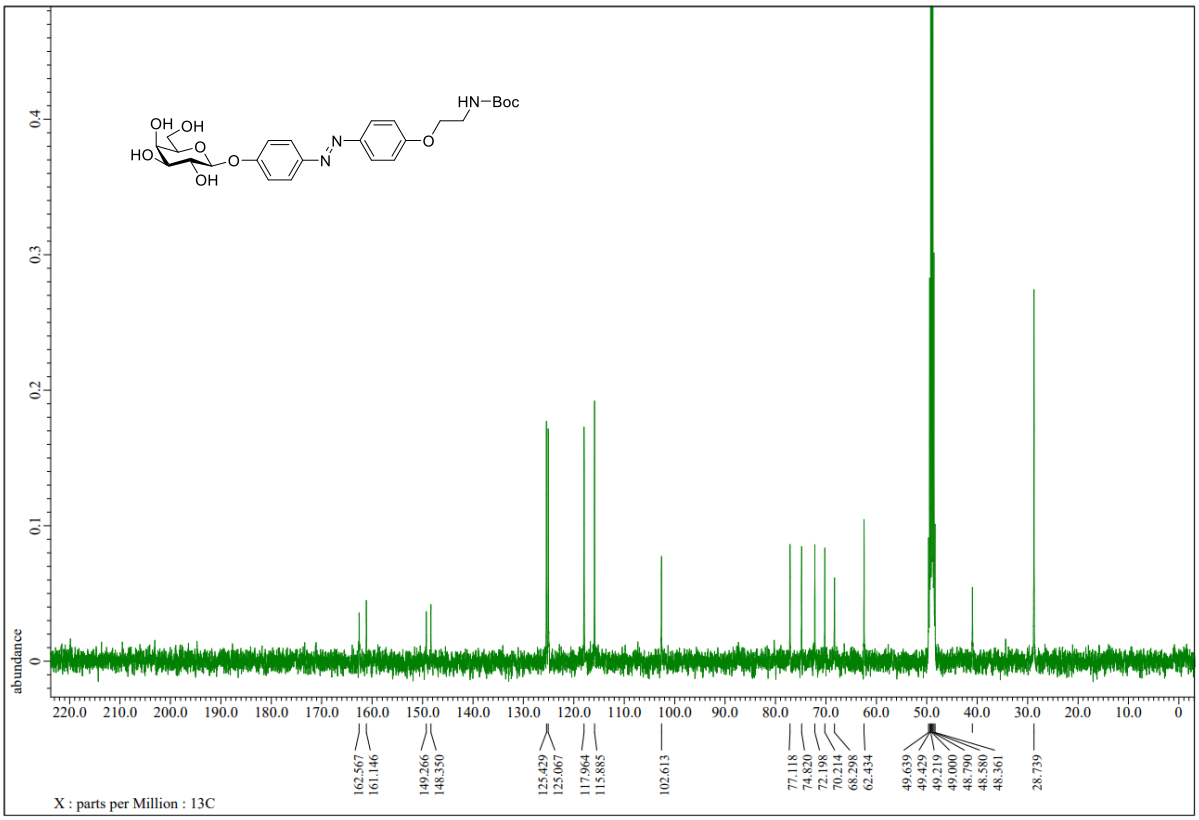

^{1}H NMR of compound *E*-10 in CD_3OD at 400 MHz

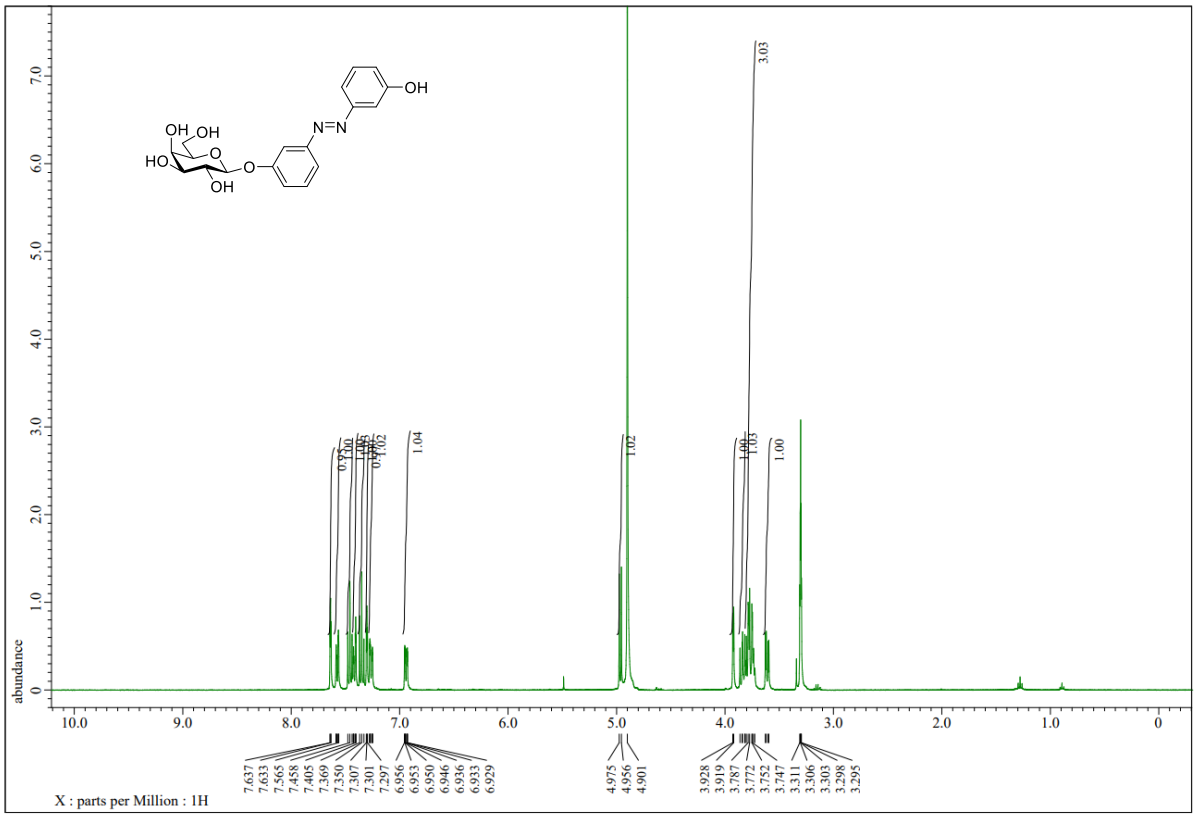

Enlarged ^{1}H NMR of compound *E*-10 in CD_3OD at 400 MHz

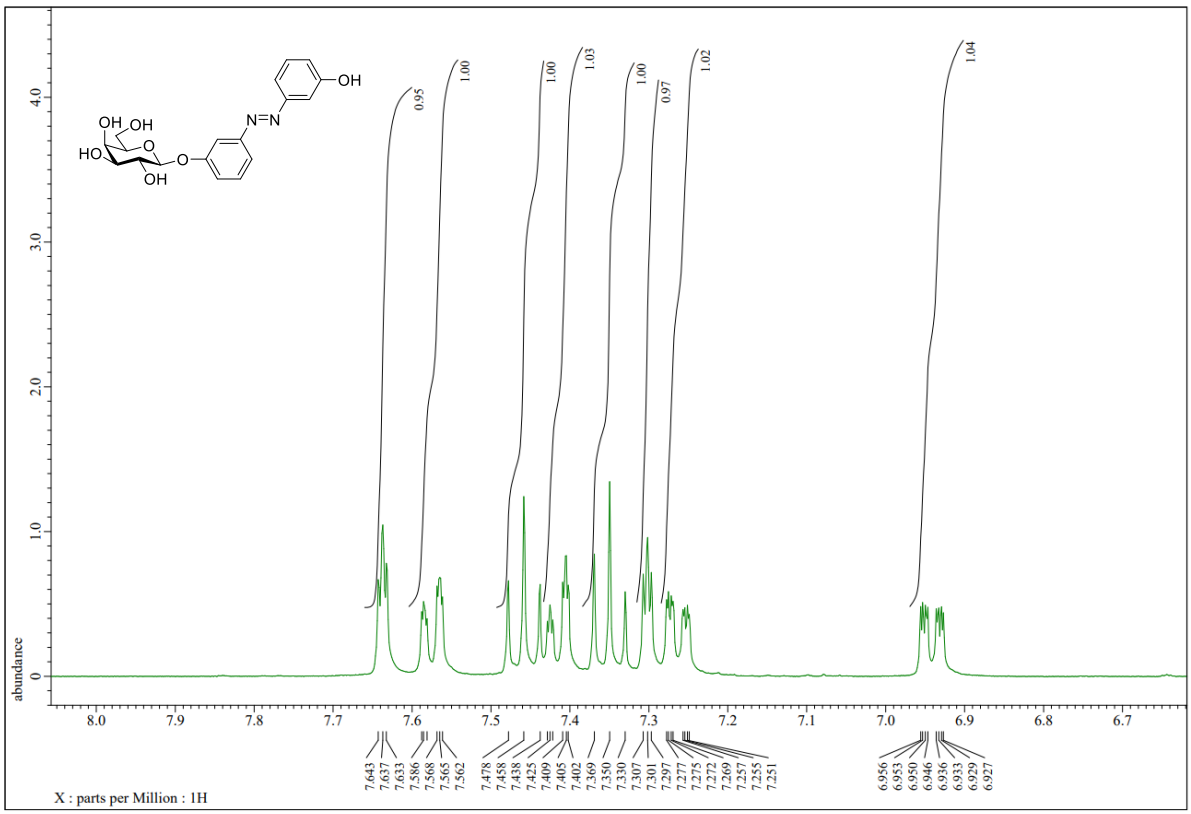

$^{13}C\{^{1}H\}$ NMR of compound *E*-10 in CD_3OD at 100 MHz

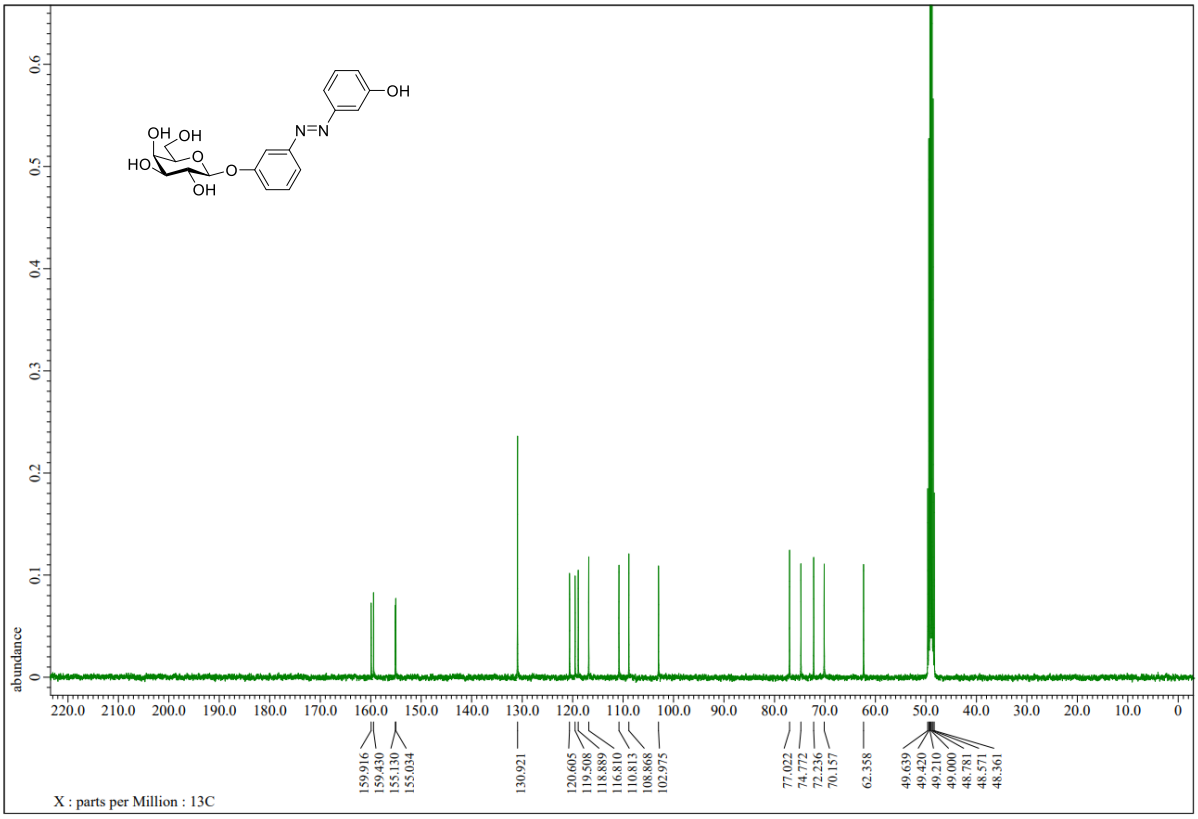

^{1}H NMR of compound *E*-11 in CD_3OD at 400 MHz

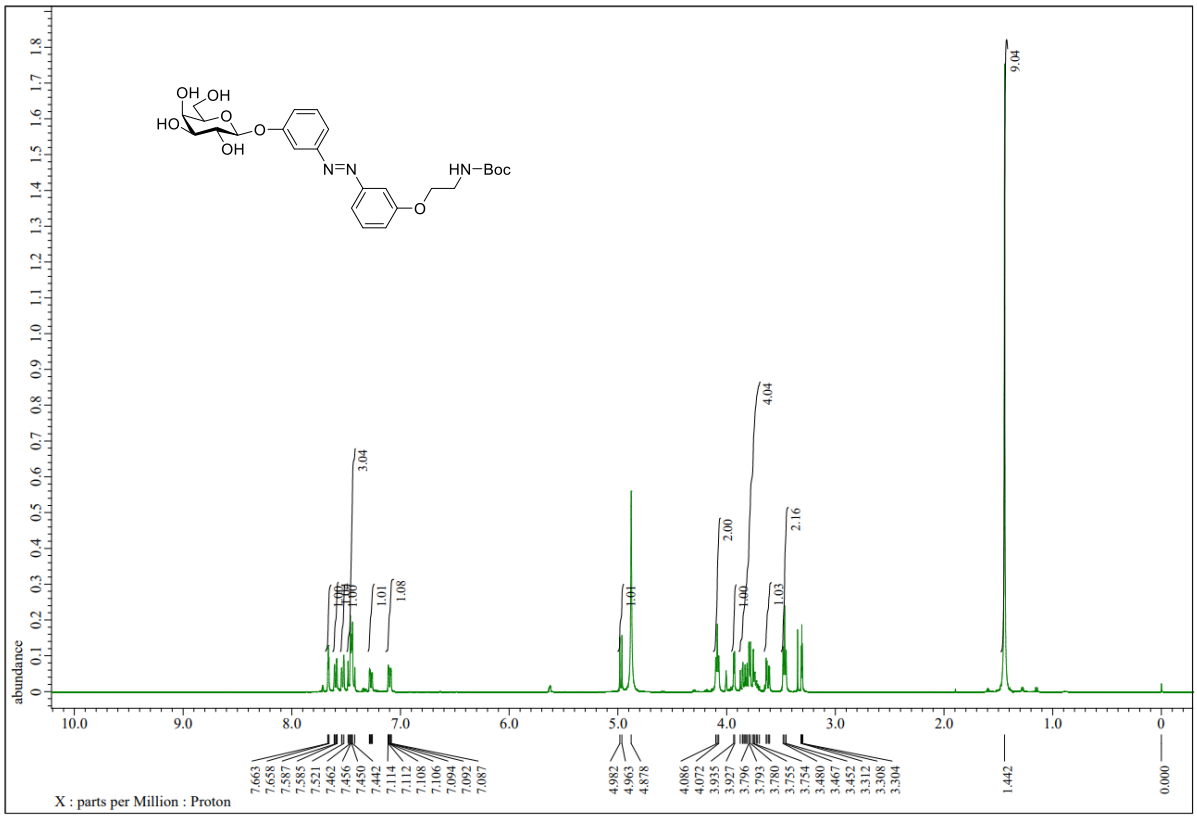

Enlarged ^{1}H NMR of compound *E*-11 in CD_3OD at 400 MHz

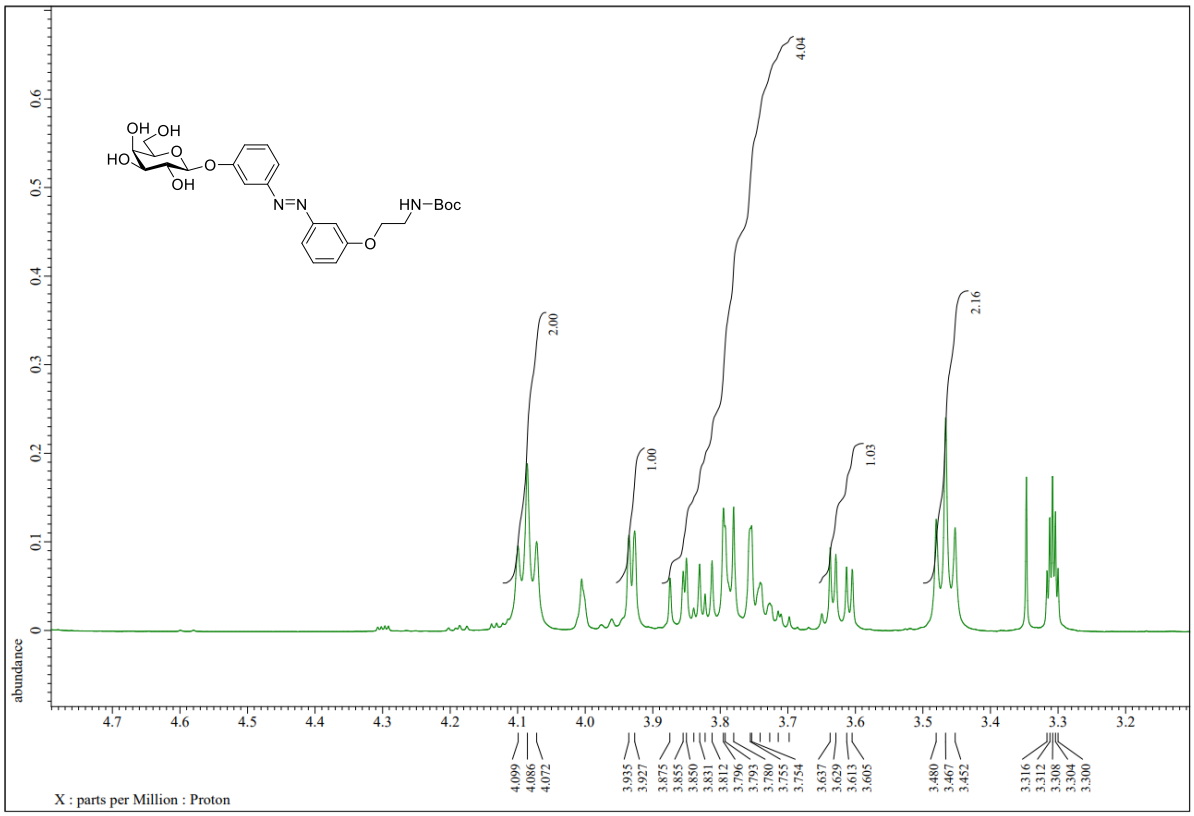

$^{13}C\{^{1}H\}$ NMR of compound *E*-11 in CD_3OD at 100 MHz

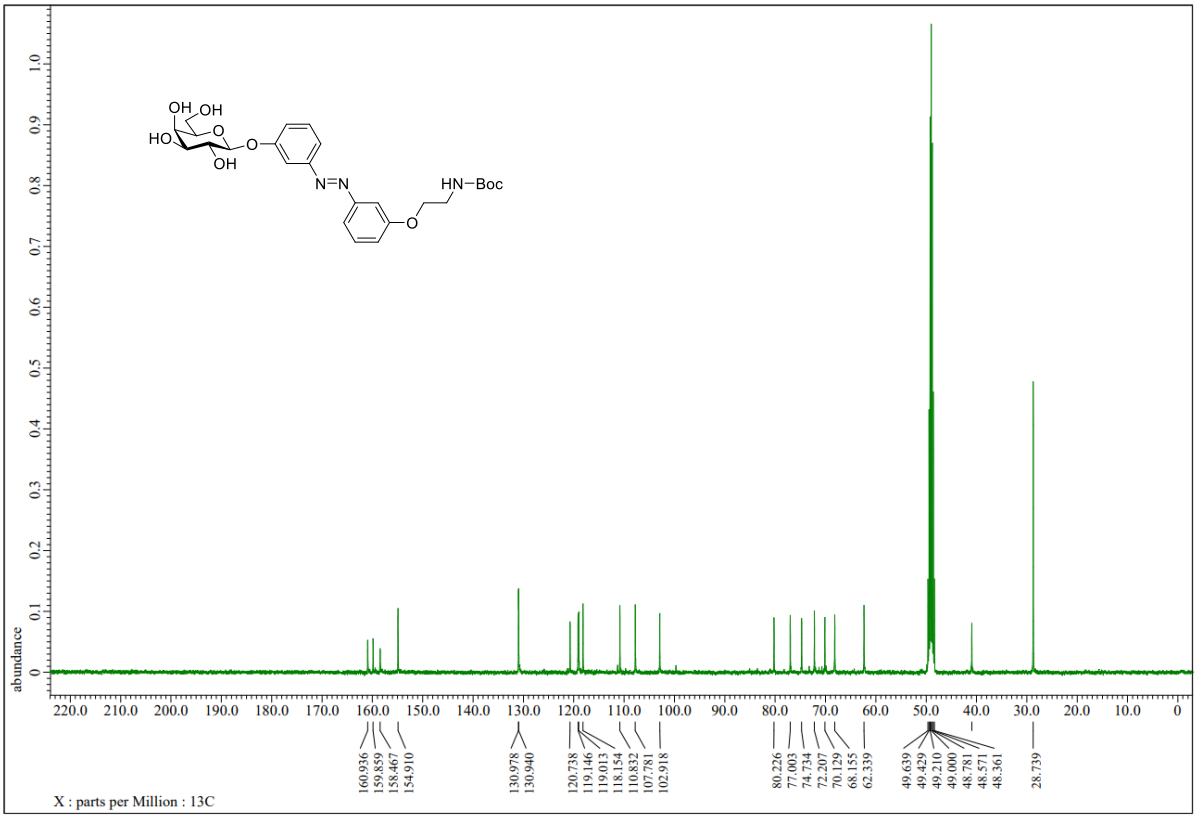

^{1}H NMR of compound *E*-14 in CD_3OD at 400 MHz

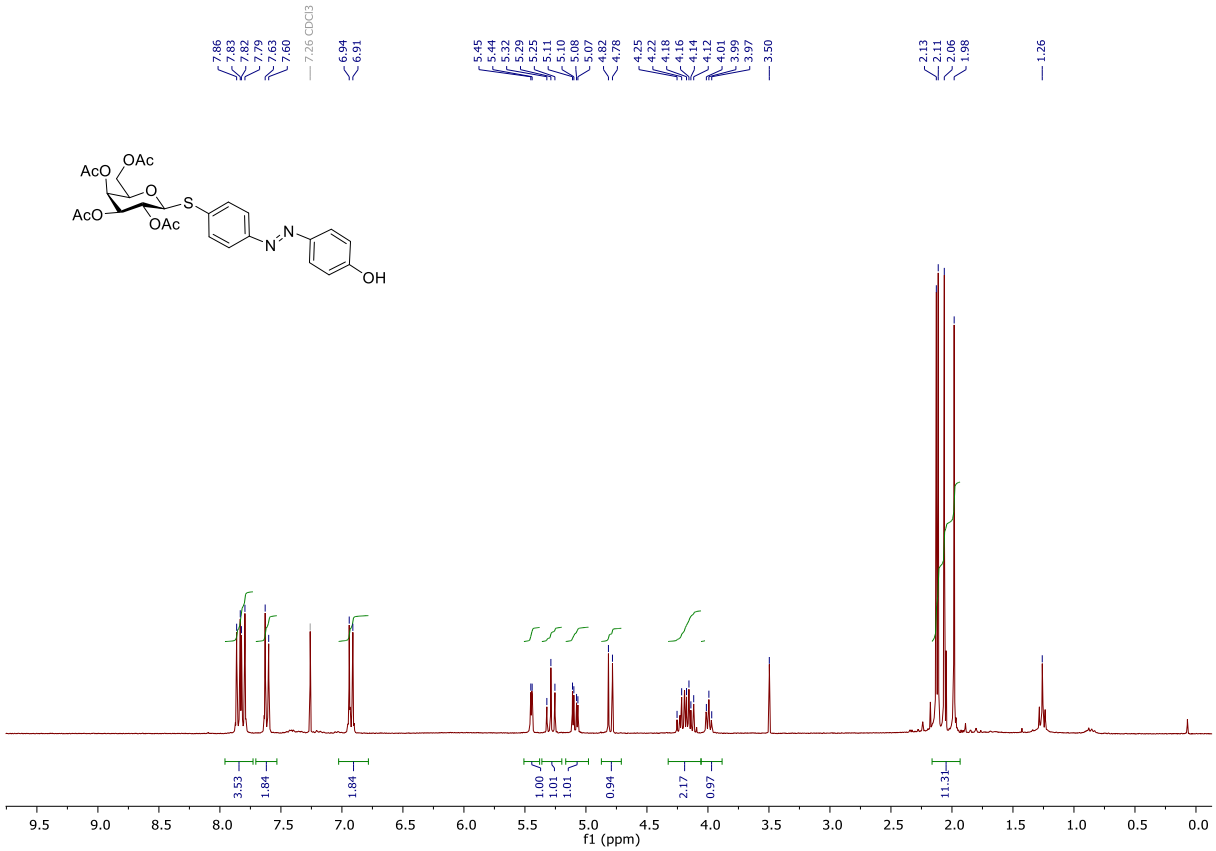

^{13}C{^{1}H} NMR of compound *E*-14 in CD_3OD at 100 MHz

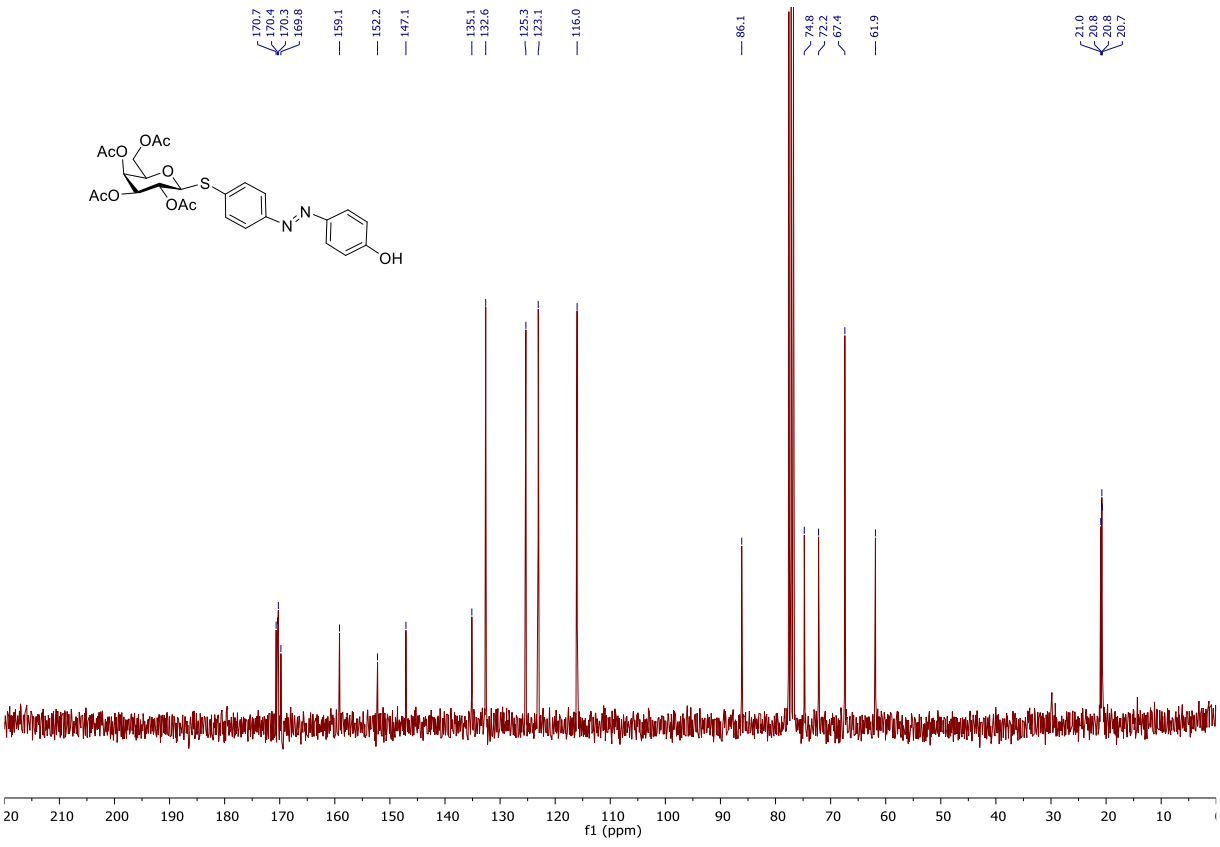

^{1}H NMR of compound *E*-15 in CD_3OD at 300 MHz

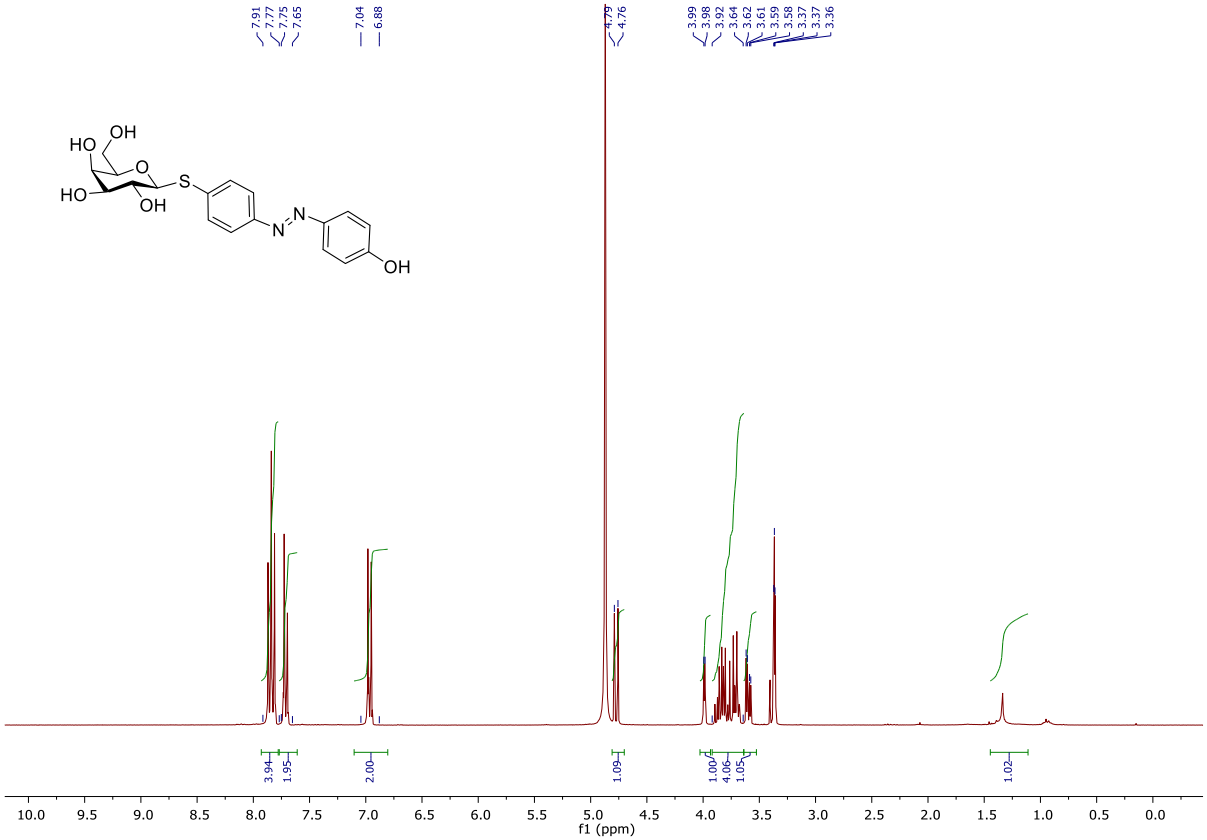

^{13}C{^{1}H} NMR of compound *E*-15 in $CDCl_3$ at 75 MHz

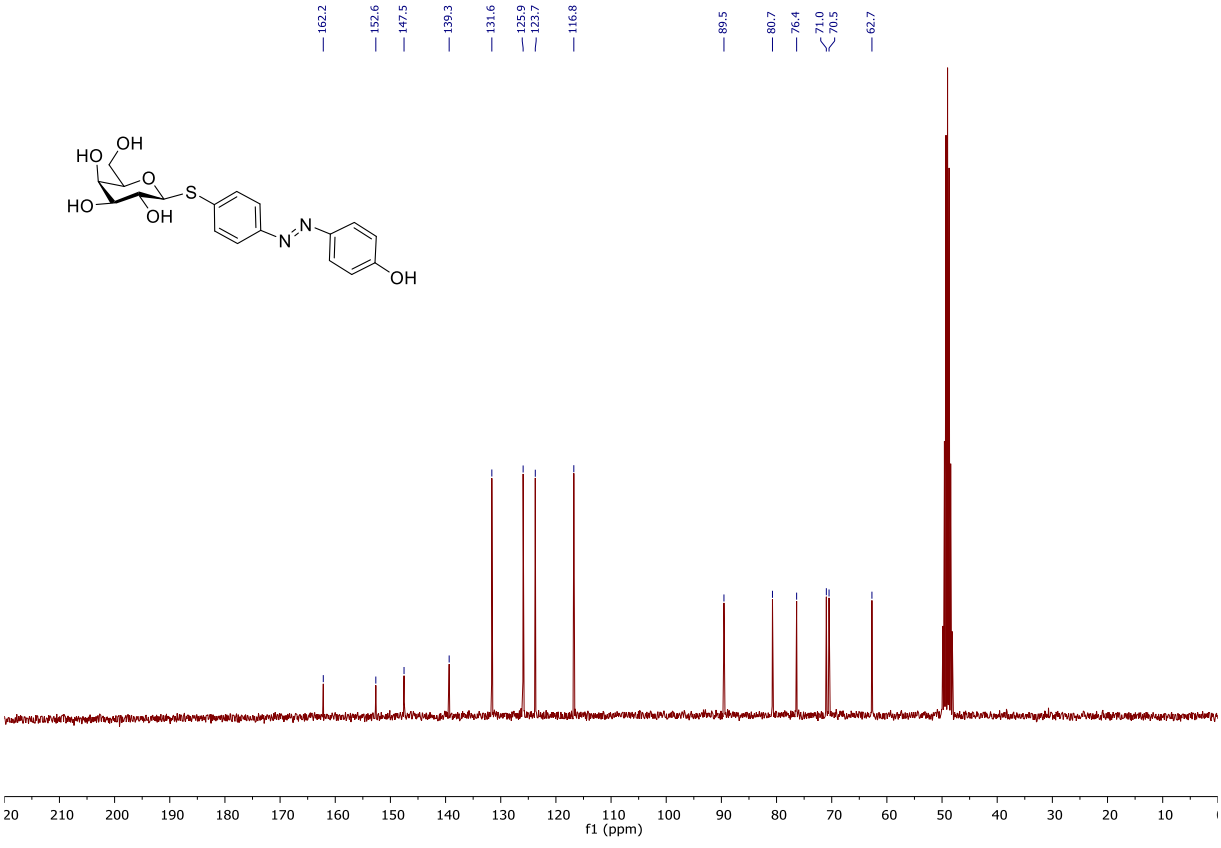

^{1}H NMR of compound *E*-16 in CD_3OD at 400 MHz

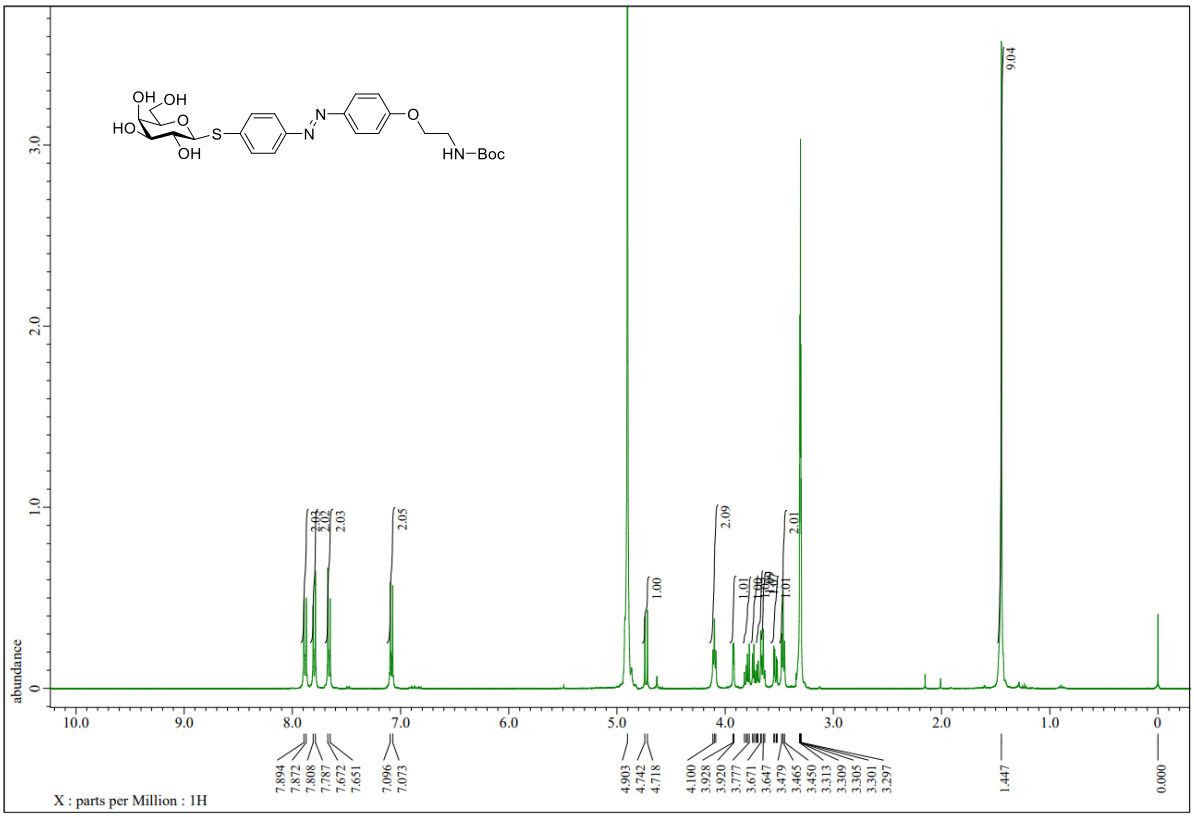

Enlarged ^{1}H NMR of compound *E*-16 in CD_3OD at 400 MHz

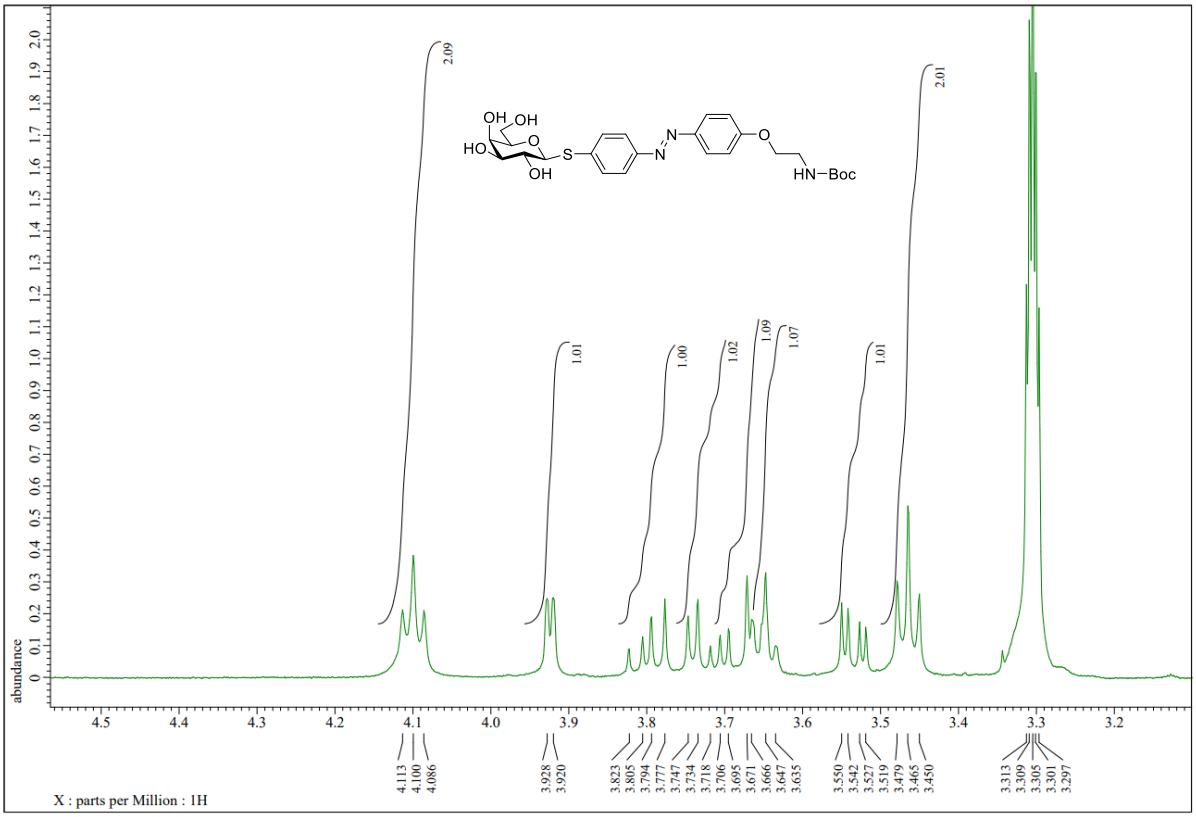

$^{13}C\{^{1}H\}$ NMR of compound *E*-16 in CD_3OD at 100 MHz

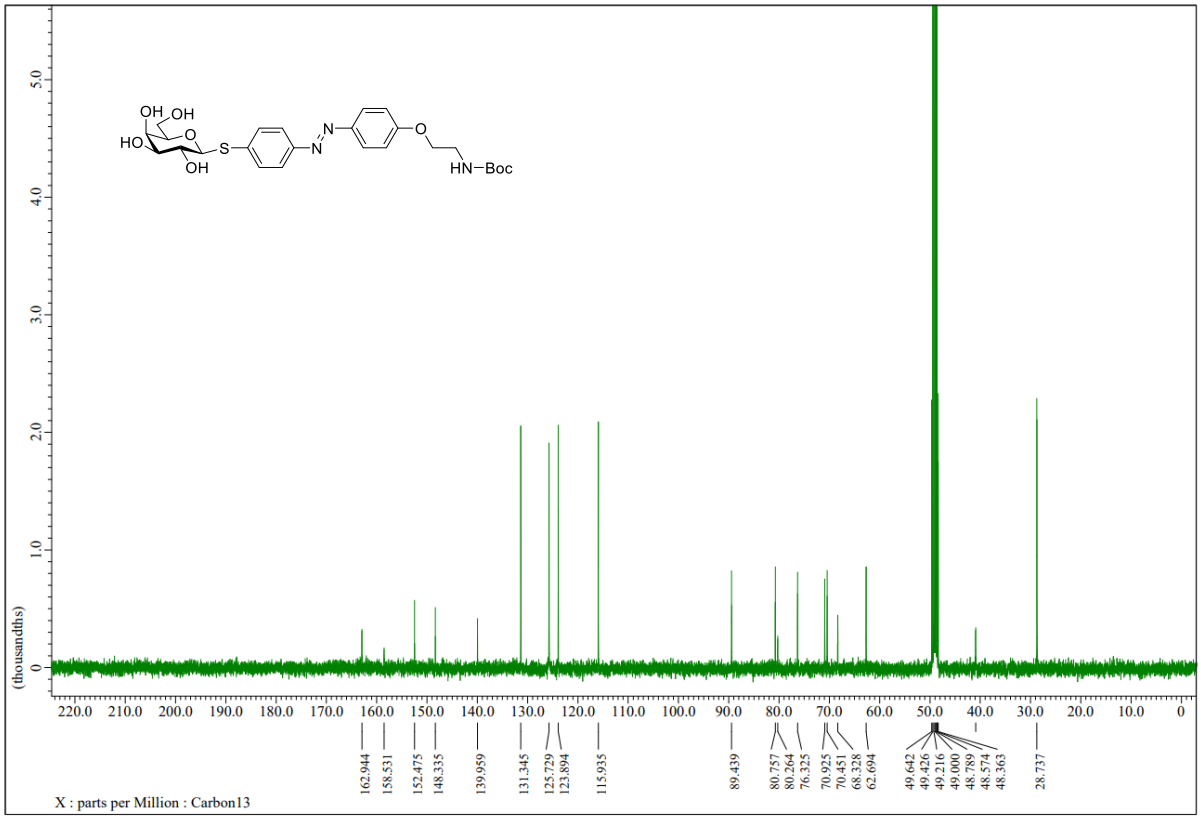

^{1}H NMR of compound *E*-18 in $CDCl_3$ at 300 MHz

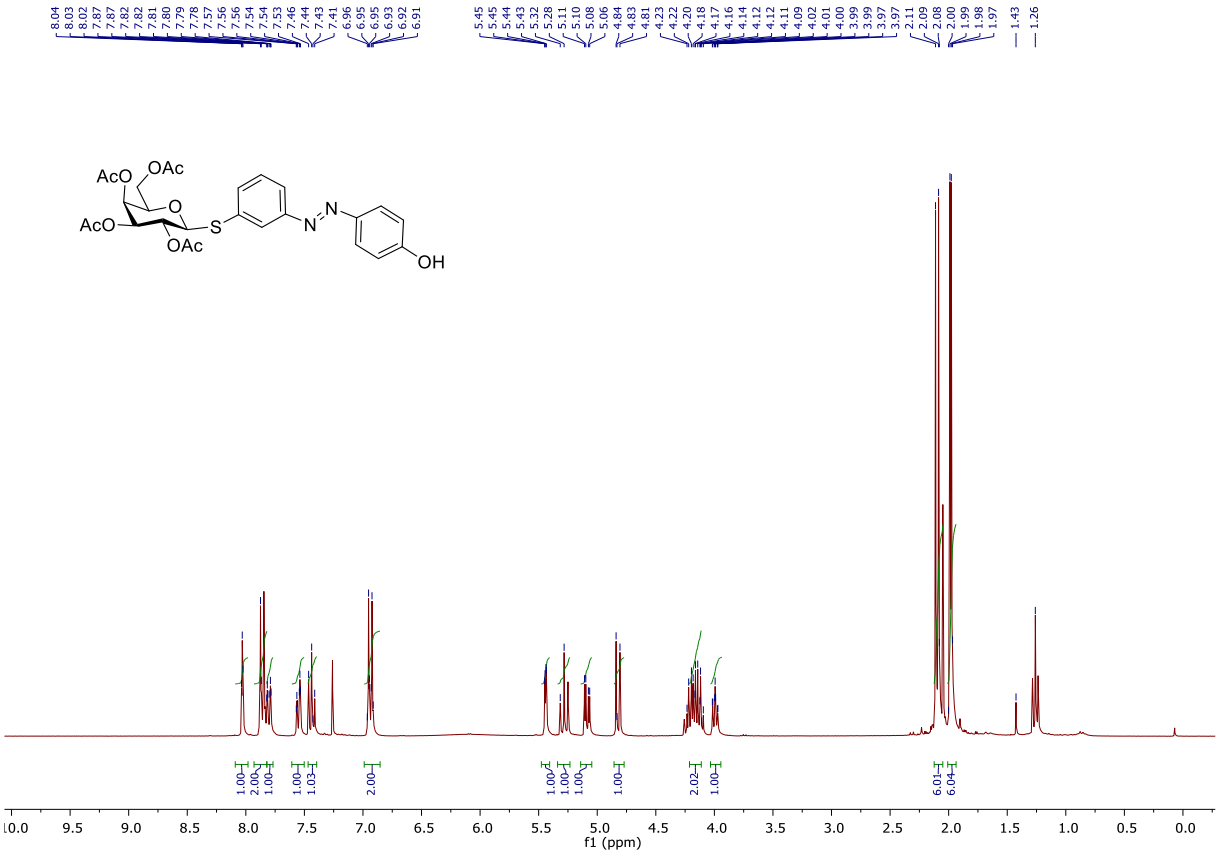

^{13}C{^{1}H} NMR of compound *E*-18 in $CDCl_3$ at 75 MHz

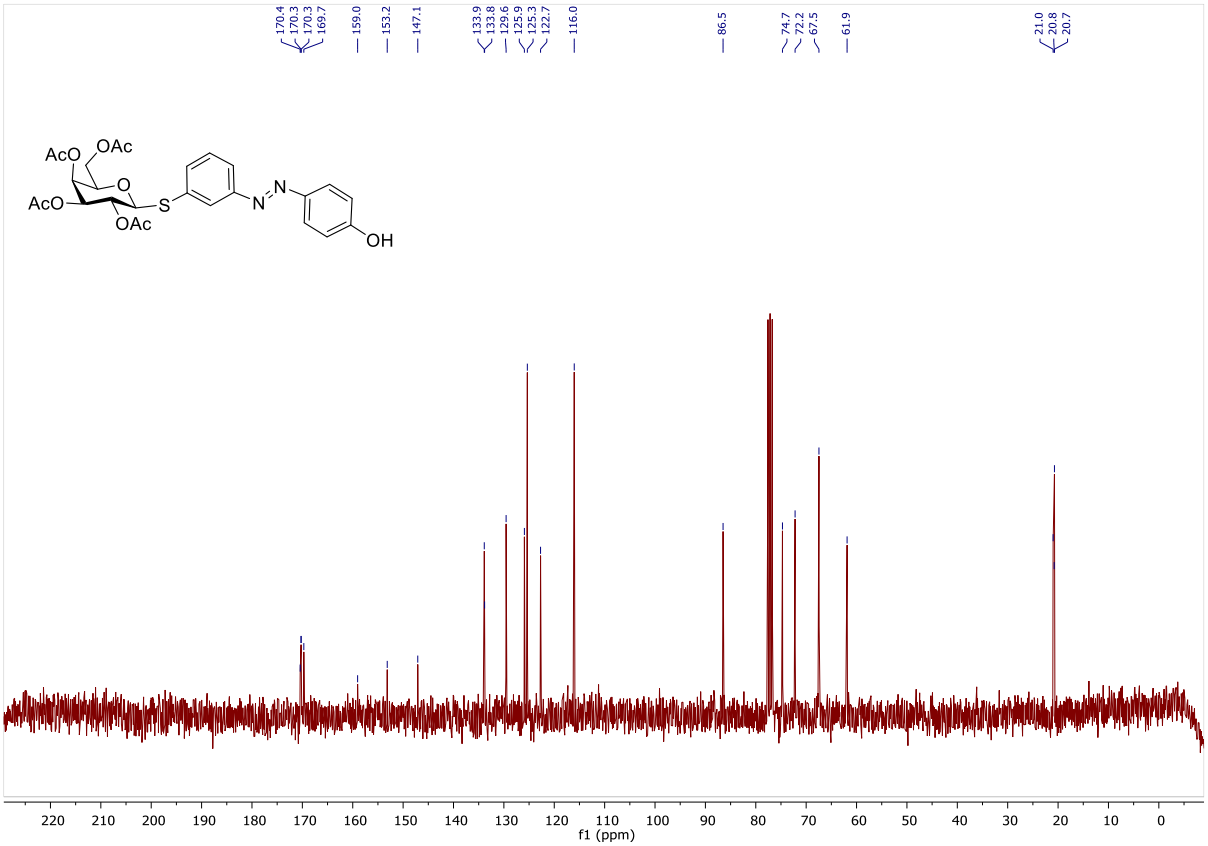

^{1}H NMR of compound *E*-19 in CD_3OD at 300 MHz

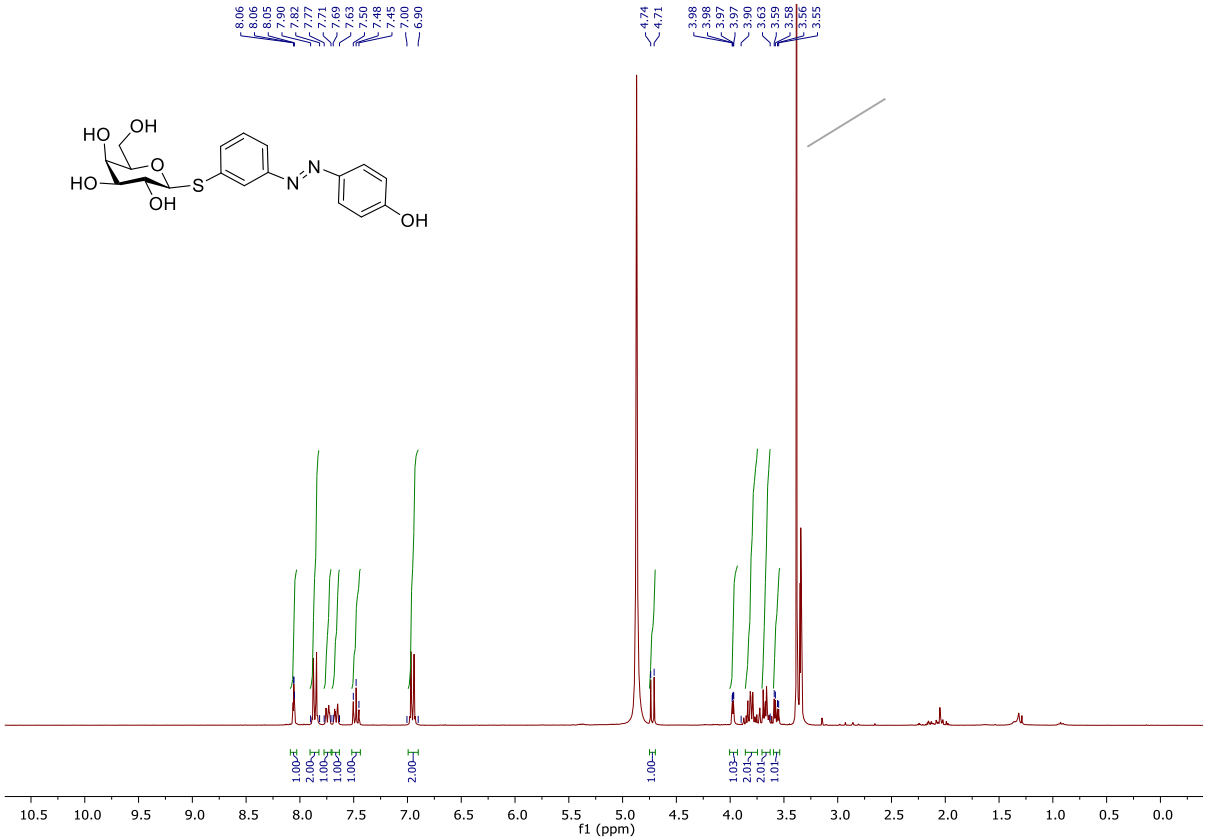

^{13}C{^{1}H} NMR of compound *E*-19 in acetone-d_6 at 75 MHz

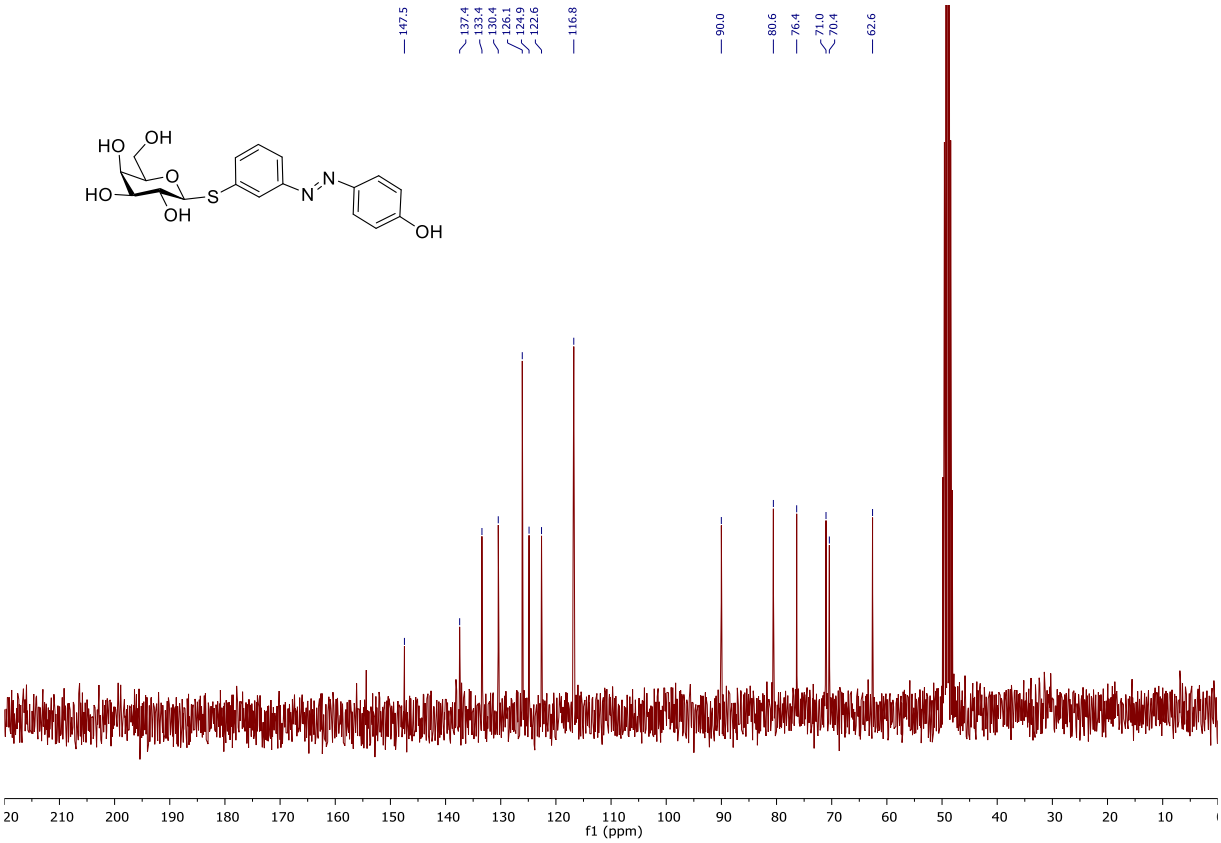

^{1}H NMR of compound *E*-20 in CD_3OD at 400 MHz

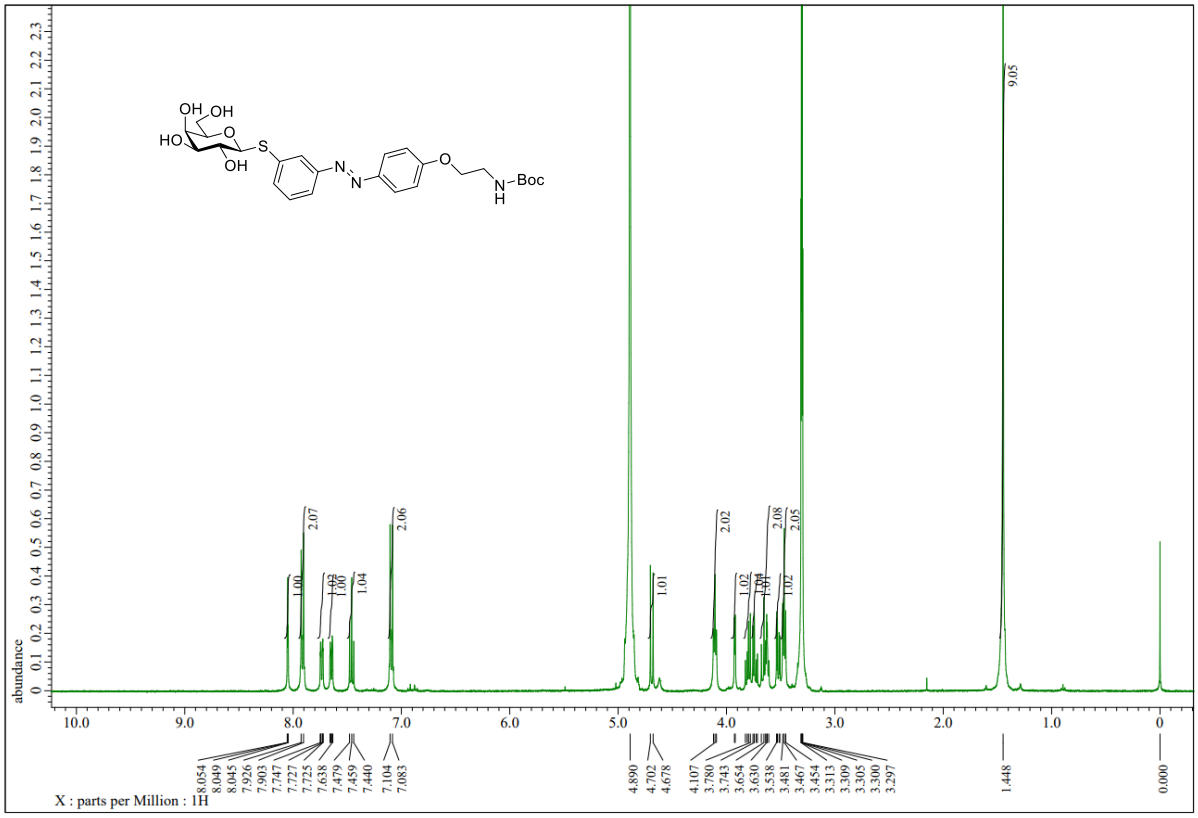

Enlarged ^{1}H NMR of compound *E*-20 in CD_3OD at 400 MHz

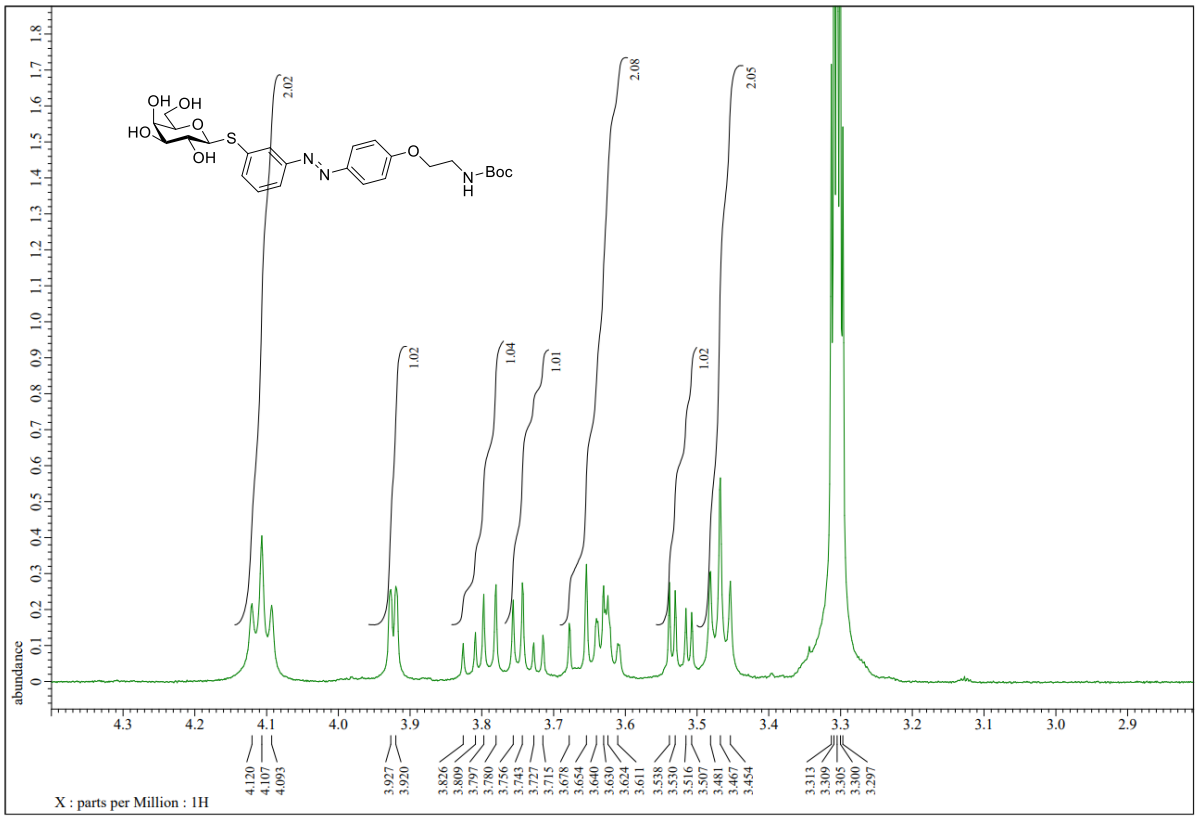

$^{13}C\{^{1}H\}$ NMR of compound *E*-20 in CD_3OD at 100 MHz

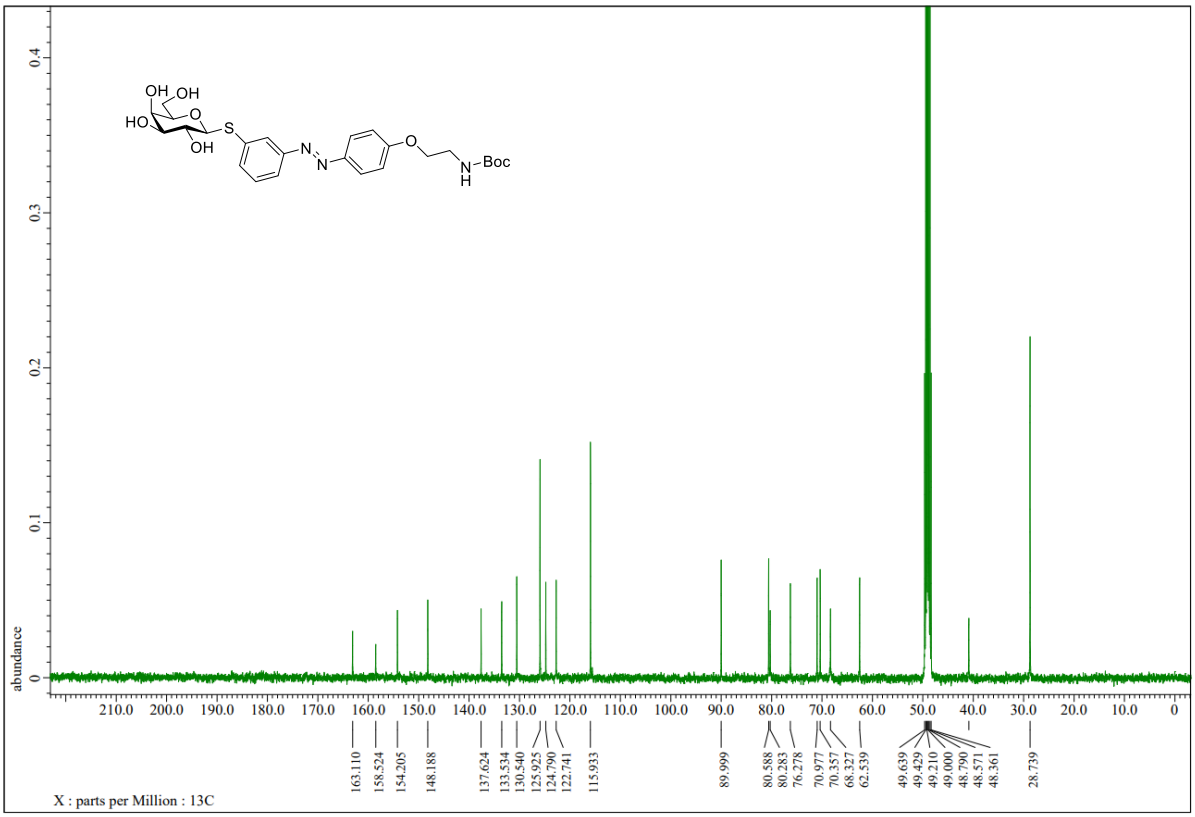

^{1}H NMR of compound *E*-22 in $CDCl_3$ at 300 MHz

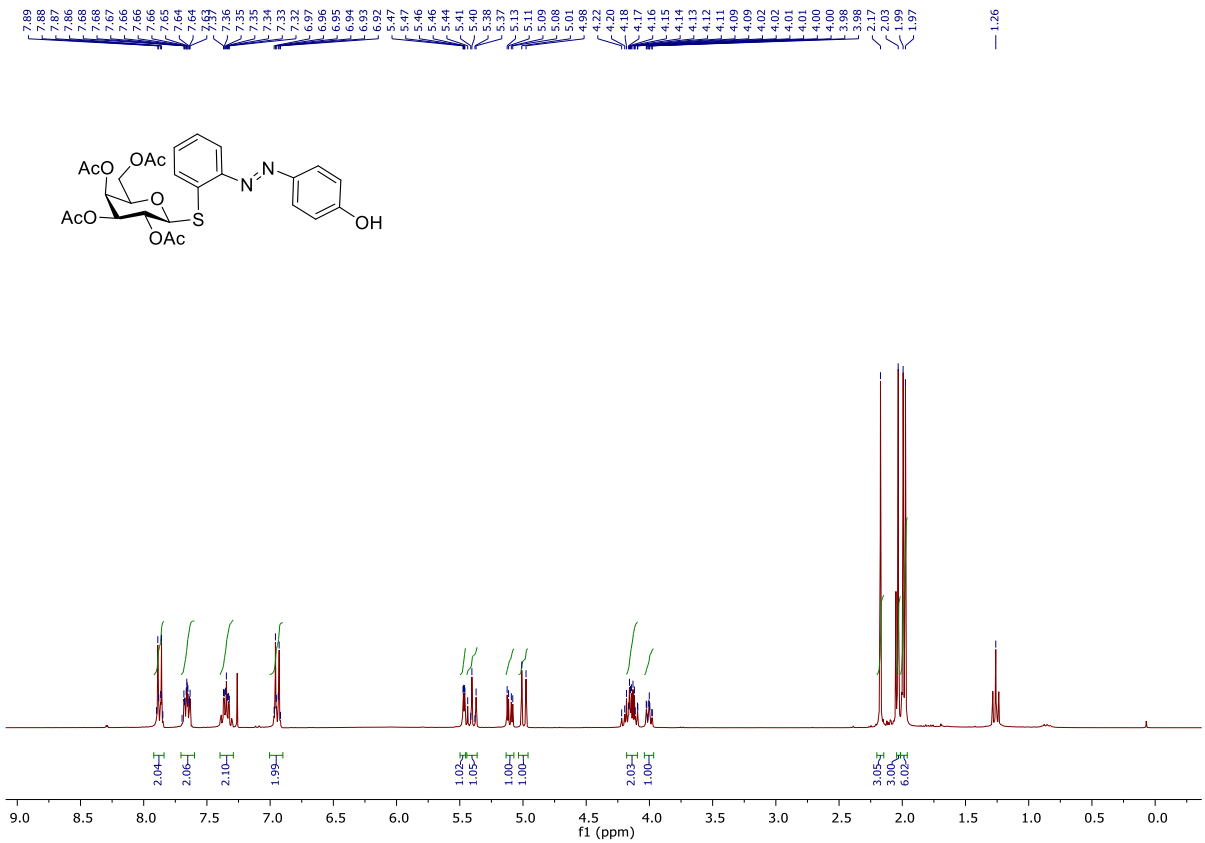

^{13}C{^{1}H} NMR of compound *E*-22 in $CDCl_3$ at 75 MHz

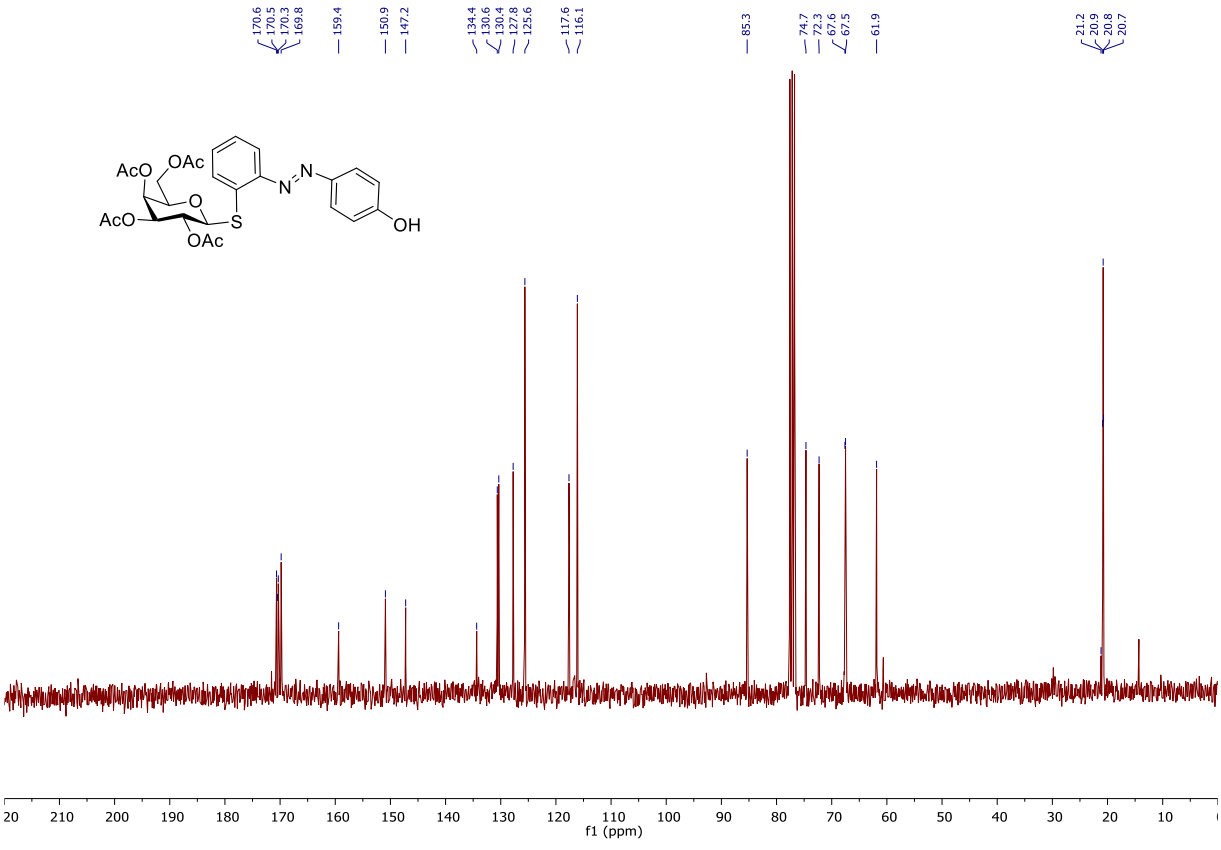

^{1}H NMR of compound *E*-23 in CD_3OD at 400 MHz

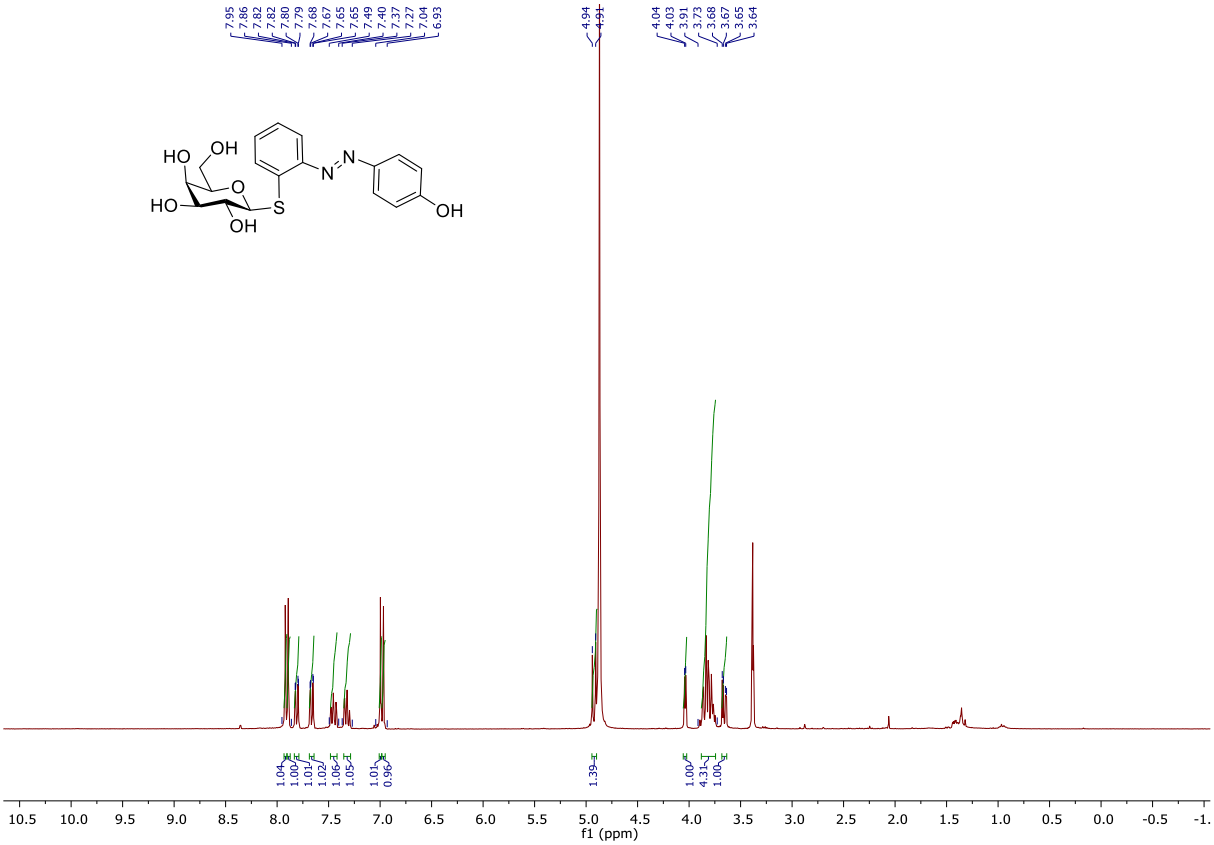

^{13}C{^{1}H} NMR of compound *E*-23 in CD_3OD at 75 MHz

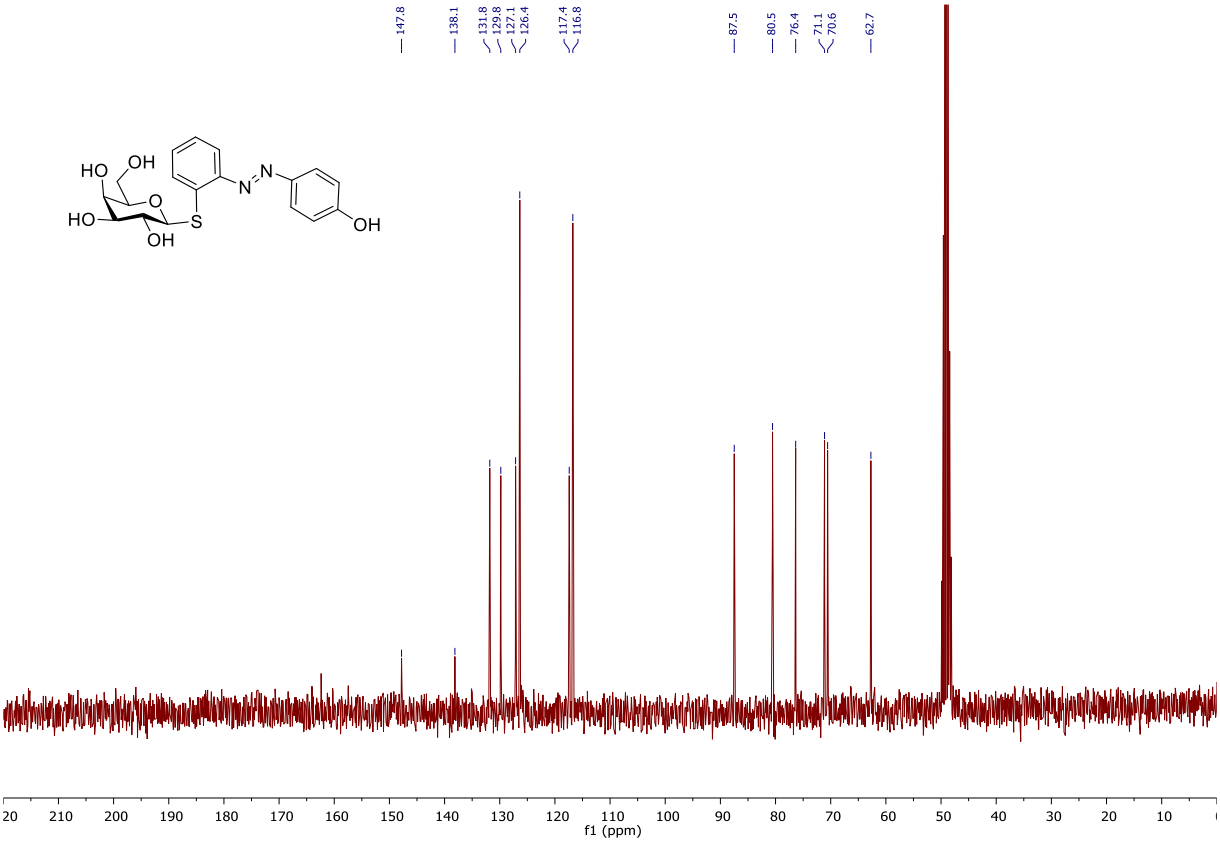

^{1}H NMR of compound *E*-24 in CD_3OD at 400 MHz

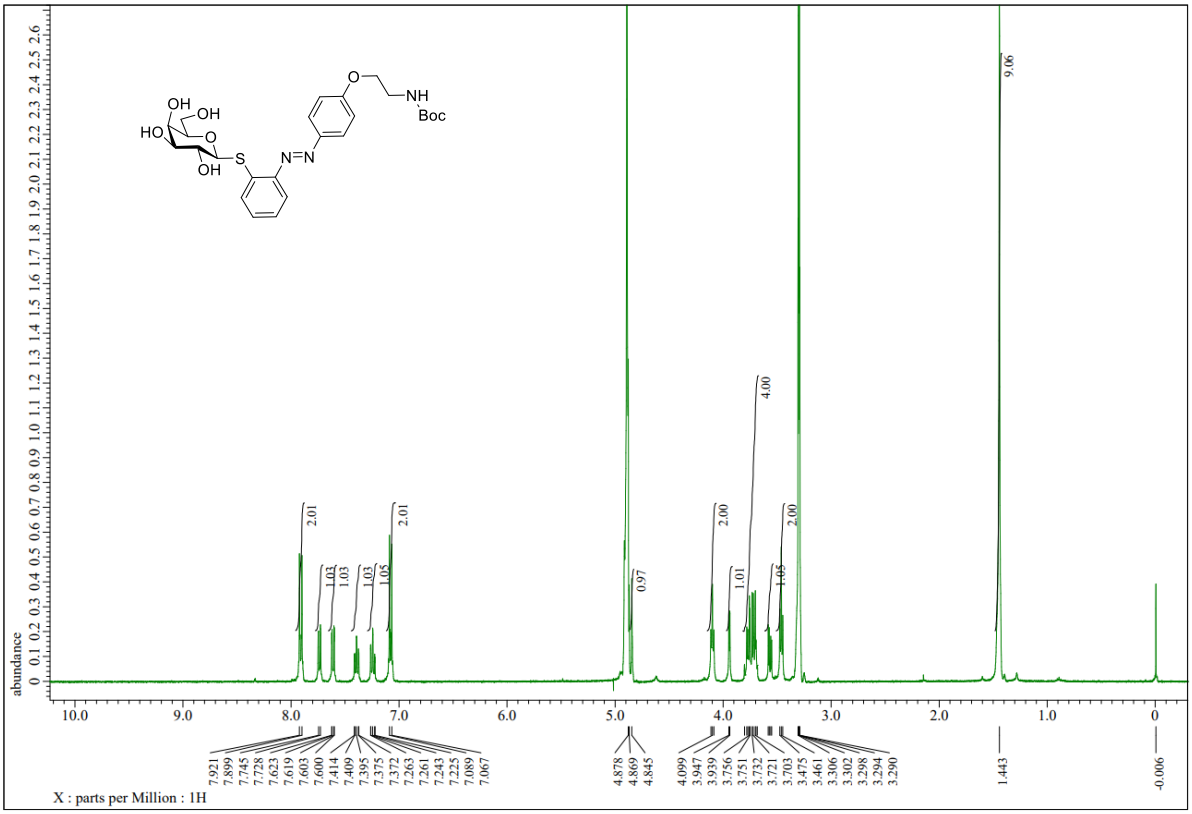

Enlarged ^{1}H NMR of compound *E*-24 in CD_3OD at 400 MHz

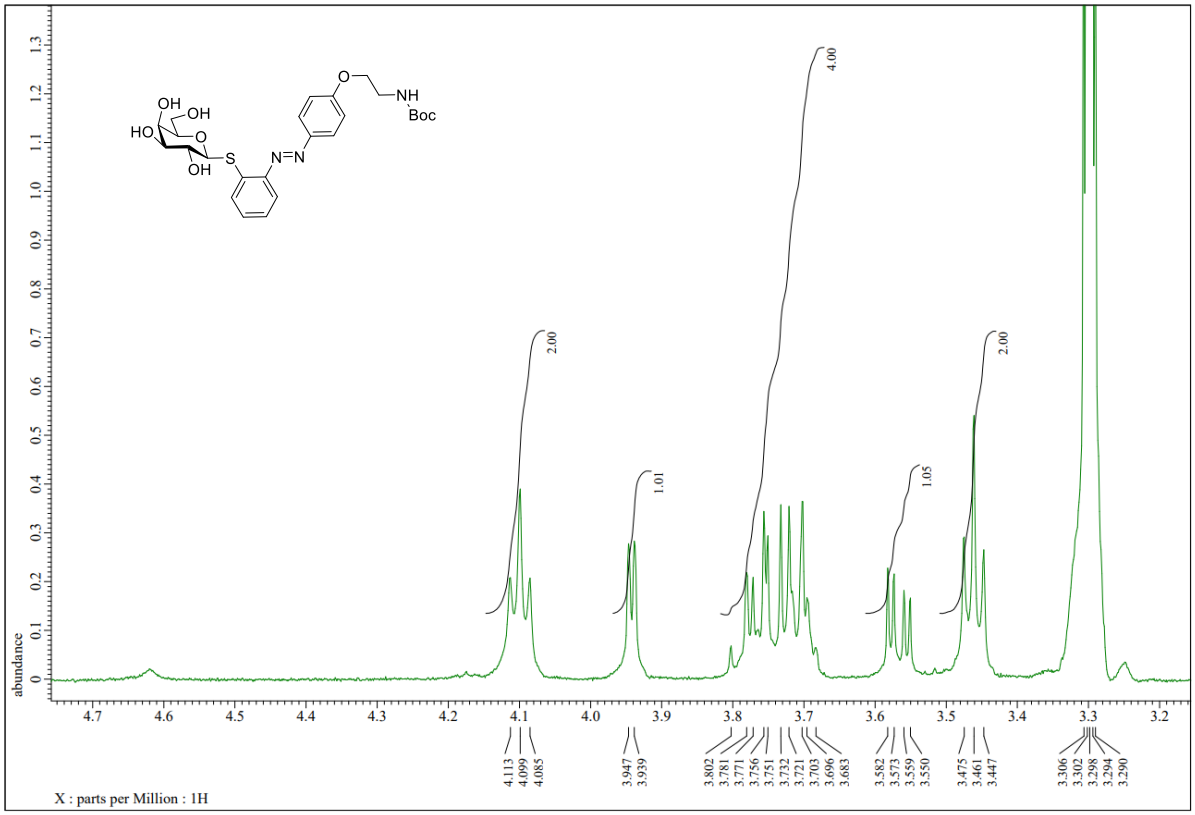

$^{13}C\{^{1}H\}$ NMR of compound *E*-24 in CD_3OD at 100 MHz